

1 **Spatial mapping of key plant functional traits in terrestrial**
2 **ecosystems across China**

3 Nannan An^{1,2,3}, Nan Lu^{2,3}, Weiliang Chen², Yongzhe Chen^{2,4}, Hao Shi^{2,3}, Fuzhong
4 Wu¹, Bojie Fu^{2,3}

5
6
7 ¹Key Laboratory for Humid Subtropical Eco-Geographical Processes of the Ministry of Education,
8 School of Geographical Sciences, Fujian Normal University, Fuzhou 350117, PR China

9 ²State Key Laboratory of Urban and Regional Ecology, Research Center for Eco-Environmental
10 Sciences, Chinese Academy of Sciences (CAS), Beijing 100085, PR China

11 ³University of Chinese Academy of Sciences, Beijing 101408, PR China

12 ⁴State Key Laboratory of Hydrosience and Engineering, Department of Hydraulic Engineering,
13 Tsinghua University, Beijing 100084, PR China

14
15 *Correspondence to:* Nan Lu (nanlv@rcees.ac.cn)

16 **Abstract**

17 Trait-based approaches are of increasing concern in predicting vegetation changes and linking
18 ecosystem structures to functions at large scales. However, a critical challenge for such approaches
19 is acquiring spatially continuous plant functional trait maps. Here, six key plant functional traits
20 were selected as they can reflect plant resource acquisition strategies and ecosystem functions,
21 including specific leaf area (SLA), leaf dry matter content (LDMC), leaf N concentration (LNC),
22 leaf P concentration (LPC), leaf area (LA) and wood density (WD). A total of 34589 in-situ trait
23 measurements of 3447 seed plant species were collected from 1430 sampling sites in China and
24 were used to generate spatial plant functional trait maps (~1 km), together with environmental
25 variables and vegetation indices based on two machine learning models (random forest and boosted
26 regression trees). The two models showed a good accuracy in estimating WD, LPC and SLA, with
27 average R^2 values ranging from 0.45 to 0.66. In contrast, both the two models had weak performance
28 in estimating LDMC, with average R^2 values below 0.25. Meanwhile, LA showed considerable
29 differences between two models in some regions. To obtain the optimal estimates, a weighted
30 average algorithm was further applied to merge the predictions of the two models to derive the final
31 spatial plant functional trait maps. Climatic effects were more important than those of edaphic
32 factors in predicting the spatial distribution of plant functional traits. Estimates of plant functional
33 traits in northeast China and the Qinghai-Tibet Plateau had relatively high uncertainties due to sparse
34 samplings, implying a need of more observations in these regions in future. Our spatial trait maps
35 could provide critical support for trait-based vegetation models and allow exploration into the
36 relationships between vegetation characteristics and ecosystem functions at large scales. The six
37 plant functional traits maps for China with 1 km spatial resolution are now available at
38 <https://figshare.com/s/c527c12d310cb8156ed2> (An et al., 2023).

39 **1 Introduction**

40 Climate change has been affecting vegetation distributions and biogeochemical cycling globally and
41 altering their feedbacks to the climate system (Kirilenko et al., 2000; Finzi et al., 2011; Jónsdóttir
42 et al., 2022). Dynamic global vegetation models (DGVMs) are powerful tools for predicting changes
43 in vegetation and ecosystem-atmosphere exchanges (e.g., water, carbon and nutrient cycling) in a
44 changing climate (Foley et al., 1996; Peng, 2000). However, conventional DGVMs are still
45 insufficient realistic, largely due to their dependence on the plant functional types (PFTs)
46 assumption (Sitch et al., 2008; Yurova and Volodin, 2011; Scheiter et al., 2013). PFTs in
47 conventional DGVMs commonly have fixed attributes (mostly trait values) (Van Bodegom et al.,
48 2012; Wullschleger et al., 2014) that do not reflect plant adaptation to environments, limiting the
49 quantification of carbon-water-nutrient feedback between terrestrial ecosystems and the atmosphere
50 (Zaehle and Friend, 2010; Liu and Yin, 2013). Trait-based approaches can provide robust theoretical
51 basis for developing the next generation of DGVMs (Van Bodegom et al., 2012; Sakschewski et al.,
52 2015; Matheny et al., 2017). Plant functional traits, which are closely associated with ecosystem
53 functions (Diaz et al., 2004; Yan et al., 2023), can effectively reflect response and adaptation of
54 plants to environmental conditions (Myers-Smith et al., 2019; Qiao et al., 2023).

55 Attempts to predict spatially continuous trait maps have been conducted at regional to global
56 scales (Madani et al., 2018; Moreno-Martínez et al., 2018; Boonman et al., 2020; Loozen et al.,
57 2020; Dong et al., 2023). Webb et al. (2010) proposed that the environment creates a filtered trait
58 distribution along an environmental gradient, and such trait-environment relationships offer
59 fundamental supports to predict the spatial distribution of plant functional traits through
60 extrapolating local trait measurements. Boonman et al. (2020) mapped the global patterns of specific
61 leaf area (SLA), leaf N concentration (LNC) and wood density (WD) based on a set of climate and
62 soil variables. As the number of available global trait databases increases (Wang et al., 2018; Kattge
63 et al., 2020), trait-environment relationships are becoming increasingly quantitative and accurate
64 (Bruehlheide et al., 2018; Myers-Smith et al., 2019). Alternatively, remote sensing approaches, such
65 as empirical methods and physical radiative transfer models (e.g., partial least squares regression,
66 PROSPECT model), have been developed to estimate plant physiological, morphological and
67 chemical traits (e.g., leaf chlorophyll content, SLA, LNC and leaf dry matter content (LDMC))
68 (Darvishzadeh et al., 2008; Romero et al., 2012; Ali et al., 2016). Vegetation indices, such as the
69 normalized difference vegetation index (NDVI) and the enhanced vegetation index (EVI), have been
70 successful in estimating plant functional traits of crops, grasslands and forests (Clevers and Gitelson,
71 2013; Li et al., 2018; Loozen et al., 2018). Loozen et al. (2020) demonstrated that EVI was the most
72 important predictor for mapping the spatial pattern of canopy nitrogen in European forests.
73 Admittedly, recent studies have suggested that combining environmental variables and vegetation
74 indices can improve the predictive accuracy of canopy nitrogen compared to those based on
75 vegetation indices alone (Loozen et al., 2020).

76 Although there have been reports on plant functional trait distribution in China in some global
77 or regional research (Yang et al., 2016; Butler et al., 2017; Madani et al., 2018; Moreno-Martínez et
78 al., 2018; Boonman et al., 2020), they are still of large uncertainties in characterizing the spatial
79 distribution of plant functional traits in China. First, global studies generally have relatively few,
80 unevenly distributed sampling sites in China (Butler et al., 2017; Madani et al., 2018; Boonman et
81 al., 2020), impeding our understanding of the true spatial characteristics of trait variability. Second,
82 the spatial pattern of traits among these studies are usually inconsistent. For example, Moreno-
83 Martínez et al. (2018) and Madani et al. (2018) demonstrated that SLA values were low in the
84 southeast areas but high in the southwest areas of China, whereas Boonman et al. (2020) found the
85 opposite. Third, most studies mainly focused on leaf traits (Yang et al., 2016; Loozen et al., 2018;
86 Moreno-Martínez et al., 2018), whereas traits associated with the whole-plant strategies, such as
87 WD, were ignored. Therefore, mapping and verifying the spatial patterns of key functional traits
88 that reflect the whole plant economics spectrum in China is a top priority.

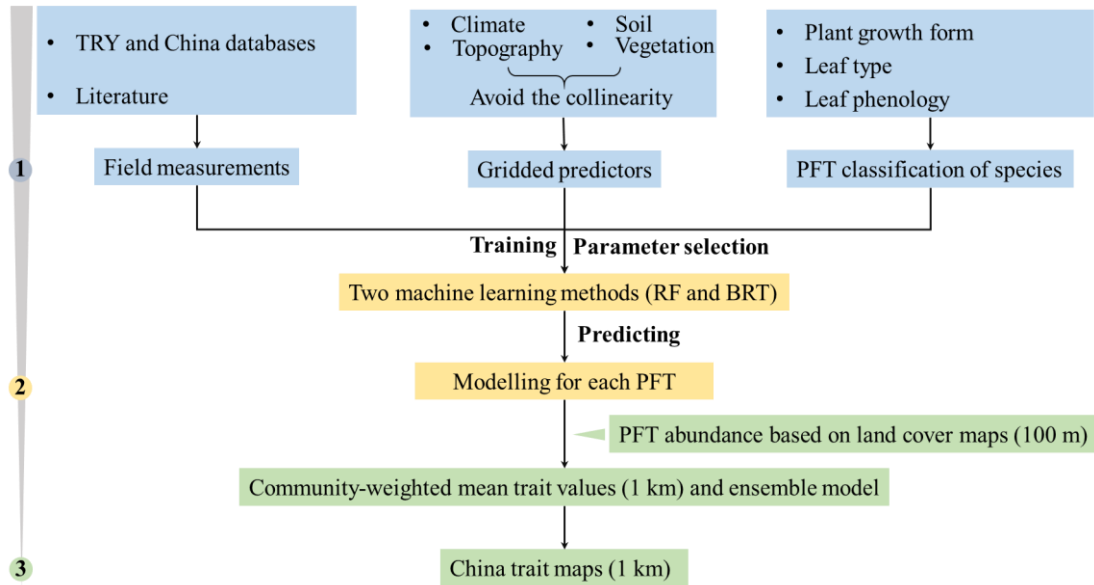
89 In this study, our main objective was to generate spatial maps for several key plant functional
90 traits, through combining field measurements, environmental variables and vegetation indices. We
91 selected six plant functional traits including SLA, LDMC, LNC, LPC, LA and WD. As key leaf
92 economics traits, SLA, LDMC, LNC and LPC were selected because they are closely linked to plant
93 growth rate, resource acquisition and ecosystem function (Wright et al., 2004; Diaz et al., 2016).
94 LA is indicative of the trade-off between carbon assimilation and water-use efficiency (Wright et
95 al., 2017), and WD reflects the trade-off between plant growth rate and support cost, with a higher
96 WD linked to a lower growth rate, a higher survival rate and a higher biomass support cost (King et
97 al., 2006). For each plant functional trait, we predicted spatial patterns at a 1 km resolution using an
98 ensemble modelling algorithm based on two machine learning methods (i.e., random forest and
99 boosted regression trees).

100 **2 Materials and Methods**

101 **2.1 Overview**

102 The spatial maps of plant functional traits in China were generated based on machine learning
103 algorithms trained by a large dataset of in-situ field measurements, environmental variables and
104 vegetation indices in three steps (Fig. 1). First, in-situ field measurements of six plant functional
105 traits were collected from TRY and China databases as well as published literature, and the PFTs of
106 plant species were classified based on plant growth form, leaf type and leaf phenology. Multiple
107 gridded predictors of climate, soil, topography and vegetation indices were used after avoiding the
108 collinearity among them. Second, random forest and boosted regression trees were used to train the
109 relationships between plant functional traits and predictors for each PFT individually. Third, the
110 spatial abundance of each PFT within 1 km grid cell was calculated using land cover map (100 m).
111 Community-weighted trait values within 1 km grid cell were calculated based on these abundances

112 of each PFT and their predicted trait values in Step 2. To reduce the variability of different single-
 113 models, we derived the final spatial maps of plant functional traits using ensemble model to merge
 114 the predictions of random forest and boosted regression trees according to their cross-validated R^2
 115 values.



116

117 **Figure 1.** Methodological workflow for spatial mapping of plant functional traits. Trait
 118 mapping is performed in three steps. Step 1: in-situ field measurement of plant functional traits, PFT
 119 classification of plant species and gridded predictors were collected. Step 2: two machine learning
 120 methods were used to predict trait values by training the field measurements and predictors for each
 121 PFT. Step 3: spatialization of trait maps by calculating the abundance of each PFT using 100 m land
 122 cover map and predicted trait values within 1 km grid cells. PFT, plant functional type; RF, random
 123 forest; BRT, boosted regression trees.

124 2.2 Plant functional trait collection and data processing

125 The information on the six plant functional traits and their ecological meanings are described
 126 in Table 1. Plant trait data was obtained and collected via two main sources. The first source was
 127 public trait databases, including the TRY database (Kattge et al., 2020) and the China Plant Trait
 128 Database (Wang et al., 2018). The second source was from literature (listed in Appendix A). To
 129 ensure data quality and comparability, we only included trait observations that met the following
 130 five criteria: 1) Measurements must be obtained from natural terrestrial fields in order to minimize
 131 the influences of management disturbance, and observations from cropland, aquatic habitat, control
 132 experiments or gardens were excluded; 2) According to the mass ratio hypothesis, the effect of plant
 133 species on ecosystem functioning is determined to an overwhelming extent by the traits and
 134 functional diversity of the dominant species and is relatively insensitive to the richness of
 135 subordinate species (Grime, 1998). Thus, we only included studies that measured plant trait
 136 observations from all species or dominant species within a community; 3) In order to consider the

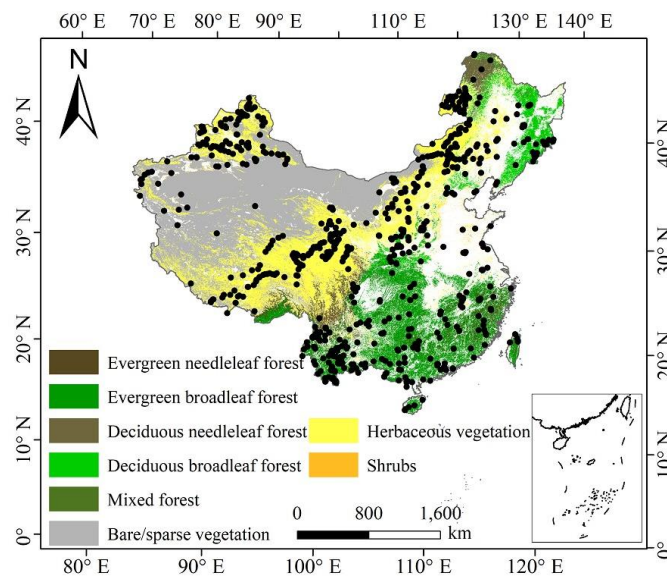
137 intraspecific trait variation, when the same species occurred in the same sampling site from different
 138 studies, we included all original observed data from different studies rather than averaging the
 139 values at the species level (Jung et al., 2010; Siefert et al., 2015); 4) Plant trait observations must be
 140 made on mature and healthy plant individuals, so some specific growth stages (e.g., seedling) and
 141 size classes (e.g., sapling) were excluded to reduce the confounding effect of ontogeny and
 142 seasonality (Thomas, 2010); 5) We only included studies with clear geographical coordinates to
 143 ensure alignment with predictor variables. The sampling location and sampling time information
 144 were also included in the dataset. The sampling time mostly focused on the growing season of a
 145 year (i.e., May-October), which ensures the relative consistency of sampling time to minimize the
 146 effects of seasonality. Plant functional traits must be sampled and measured according to
 147 standardized measurement procedures (Perez-Harguindeguy et al., 2013) to reduce the variation and
 148 uncertainty among different data sources. In this study, we included SLA measurements on sun-
 149 leaves, and WD measurements on both heartwood and sapwood of tree species.

150 **Table 1** Description of plant functional traits selected in this study and their relevant ecosystem
 151 functions.

Trait	Abbreviation	Description	Relevant ecosystem functions
Specific leaf area	SLA	As a core leaf economics trait (Wright et al., 2004), it is related to trade-off between leaf lifespan and C acquisition as well as light competition (Reich et al., 1991)	Productivity, litter decomposition, competitive ability (Bakker et al., 2011; Smart et al., 2017)
Leaf dry matter content	LDMC	Strongly related to resource availability and potential growth rate (Hodgson et al., 2011)	Productivity, litter decomposition, herbivore resistance, and drought tolerance (Bakker et al., 2011; Smart et al., 2017; Blumenthal et al., 2020)
Leaf N concentration	LNC	As a core leaf economics trait, it is strongly related to photosynthetic capacity (Wright et al., 2004)	Productivity, nutrient cycling, litter decomposition (LeBauer and Treseder, 2008; Bakker et al., 2011)
Leaf P concentration	LPC	As a core leaf economics trait, it is strongly related to photosynthetic capacity (Wright et al., 2004)	Productivity, nutrient cycling, litter decomposition (LeBauer and Treseder, 2008; Bakker et al., 2011)
Leaf area	LA	Trade-off between C assimilation and water use efficiency, it is related to energy balance (Wright et al., 2017)	Productivity (Li et al., 2020)
Wood density	WD	A measure of carbon investment, representing the trade-off between growth and mechanical support (Martínez-Vilalta et al., 2010)	Drought tolerance, productivity (Hoeber et al., 2014; Liang et al., 2021)

152 The plant trait data was checked for possible errors and corrected in three steps as follows.
 153 First, species name and taxonomic nomenclature were corrected and standardized according to the
 154 Plant List (<http://www.theplantlist.org/>) using the “plantlist” package. Second, illogical values,
 155 repeated values and outliers were removed, which were defined by observations exceeding 1.5
 156 standard deviations of the mean trait value for a given species (Kattge et al., 2011). Third, we

157 appended information on plant growth form, leaf type and leaf phenology from the TRY categorical
 158 traits database (<https://www.try-db.org/TryWeb/Data.php#3>) and *Flora Reipublicae Popularis*
 159 *Sinicae* (<http://www.iplant.cn/frps>), which were used to match species names to PFTs. We associated
 160 each species with a corresponding PFT based on plant growth form (tree, shrub and grass), leaf type
 161 (broadleaf and needleleaf) and leaf phenology (evergreen and deciduous). For example, the
 162 information on *Salix matsudana* is: tree, deciduous and broadleaf, thus, we were able to associate
 163 the PFT of deciduous broadleaf forest (DBF) to this species. The species that did not correspond to
 164 any PFT were discarded. After these treatments, we collected a total of 34589 trait measurements
 165 from 1430 sampling sites for our database, representing 3447 species from 195 families and 1066
 166 genera (Fig. 2 and Fig. B1 in Appendix B). Information on the statistics for the six plant functional
 167 traits collected in this study is shown in Table B1 in Appendix B.
 168



169
 170 **Figure 2.** Location distribution and land cover map in China.

171 2.3 Preparing predictor variables

172 2.3.1 Climate data

173 Twenty-one climate variables were used in this study, including 19 bioclimate variables, solar
 174 radiation (RAD) and aridity index (AI) (Table B2 in Appendix B). The 19 bioclimate variables and
 175 RAD were obtained from the WorldClim version 2.1 for the period from 1970 to 2000
 176 (<https://www.worldclim.org/data/worldclim21.html>). The AI data was extracted from the CGIAR
 177 Consortium of Spatial Information (CGIAR-CSI) website for the period from 1970 to 2000
 178 (<http://www.csi.cgiar.org>) (Trabucco and Zomer, 2018). The spatial resolution of climate data is 1
 179 km.

180 2.3.2 Soil data

181 Twelve soil variables were included in this study, representing the different aspects of soil properties,
 182 i.e. soil texture, bulk density (BD), pH and soil nutrients (Table B2 in Appendix B). All soil variables
 183 were extracted from the Soil Database of China for Land Surface Modeling

184 (<http://globalchange.bnu.edu.cn/research/soil2>) (Shangguan et al., 2013). Given the importance of
185 topsoil properties on community composition (Bohner, 2005), we averaged the first four layers to
186 represent the topsoil properties (~ 30 cm) in our study. The spatial resolution is 1 km.

187 **2.3.3 Topography**

188 The topographic variable was elevation. Elevation data was extracted from the STRM 90m dataset
189 in China, based on the SRTM V4.1 database (<https://www.resdc.cn/data.aspx?DATAID=123>). The
190 spatial resolution is 1 km.

191 Given the collinearity among climate and soil variables, we reduced the number of
192 environmental predictors based on Pearson's correlation coefficient (r) (Figs. B2 and B3 in
193 Appendix B). Among a set of highly correlated variables ($r > 0.75$), only one variable was retained
194 in subsequent analysis to ensure a combination of different environmental variables. The final
195 selection of environment predictors included nineteen variables: mean annual temperature (MAT),
196 mean diurnal range (MDR), min temperature of coldest quarter (T_{min}), max temperature of warmest
197 quarter (T_{max}), temperature seasonality (TS), mean annual precipitation (MAP), precipitation
198 seasonality (PS), precipitation of wettest quarter (PEQ), precipitation of driest quarter (PDQ), AI,
199 RAD, elevation, soil sand content (SAND), pH, BD, soil total N (STN), soil total P (STP), soil
200 available P (SAP), soil alkali-hydrolysable N (SAN) and cation exchange capacity (CEC).

201 **2.3.4 Vegetation indices**

202 Three categories of vegetation indices were included in this study (Table B2 in Appendix B). First,
203 EVI was extracted from the MOD13A3 V006 product
204 (<https://lpdaac.usgs.gov/products/mod13a3v006/>). This product is available as a monthly average
205 with spatial resolution of 1 km, ranging from January 2000 to December 2018. Second, MODIS
206 reflectance data was also extracted from the MOD13A3 V006 product, including MIR reflectance,
207 NIR reflectance, red reflectance and blue reflectance. Third, the MERIS terrestrial chlorophyll index
208 (MTCI) was extracted from the Natural Environment Research Council Earth Observation Data
209 Centre (NERC-NEODC, 2005) (<https://data.ceda.ac.uk/>). MTCI data is available globally as a
210 monthly average at 4.63 km spatial resolution, and ranges from June 2002 to December 2011. It is
211 noted that valid MTCI values should be greater than 1, so our study deleted any values less than 1.

212 To avoid collinearity, we also reduced the number of vegetation indices based on Pearson's
213 correlation coefficient (r) (Fig. B4 in Appendix B). Most selected variables were related to growing
214 seasons due that plant functional traits were measured during the growing season. Furthermore,
215 based on the results of Pearson's correlation coefficient (r), MTCI, MIR, NIR, red and blue in
216 January showed low correlations with those in growing season, thus they were included in
217 subsequent analysis. The final selection included 36 variables: annual EVI, EVI (May, June, July,
218 August and September), MTCI, MIR, NIR, red and blue (all for January, June, July, August and
219 September).

220 Both environmental variables and vegetation indices variables were resampled to a consistent
221 spatial resolution of 1 km using the nearest neighborhood method.

222 PFT is also an important factor in influencing the variation of plant functional traits (Verheijen
223 et al., 2016; Loozen et al., 2020), thus the trait predictions were performed for each PFT individually.
224 We used the 2015 land cover map at a 100 m spatial resolution to calculate the relative abundance
225 of each PFT within 1 km grid cells, which was extracted from the Copernicus Global Land Service
226 (CGLS-LC100, Version 3) (<https://land.copernicus.eu/global/products/lc>) (Buchhorn et al., 2020).
227 We focused on natural terrestrial vegetation, so all artificial or crop areas were thus eliminated in
228 our dataset. Seven categories were included: evergreen needleleaf forest (ENF), evergreen broadleaf
229 forest (EBF), deciduous needleleaf forest (DNF), deciduous broadleaf forest (DBF), shrubland
230 (SHL), grassland (GRL) and bare/sparse vegetation.

231 **2.4 Model fitting and validation**

232 To predict spatial patterns of plant functional traits, we used two machine learning models, i.e.,
233 random forest and boosted regression trees.

234 Random forest is an ensemble machine learning method based on classification and regression
235 trees using collections of regression trees to classify observations according to a set of predictive
236 variables (Breiman, 2001). This method repeatedly constructs a set of trees from random samples
237 of training data, and the final prediction is produced by integrating the results of all individual trees,
238 which makes it a robust method. The model is controlled by two main parameters: the number of
239 sampled variables (mtry) and the number of trees (ntree). The mtry was set to range from 1 to 57 (at
240 an interval of 1), and the ntree was set as 500, 1000, 2000, 5000 and 10000 in subsequent runs. This
241 analysis was performed using the ‘randomForest’ function in the ‘randomForest’ package (Liaw and
242 Wiener, 2002).

243 Boosted regression trees are machine learning methods based on generalized boosted
244 regression models and using a boosting algorithm to combine many sample tree models to optimize
245 predictive performance (Elith et al., 2006). There is no need for prior data transformation or the
246 elimination of outliers, and this method can fit complex non-linear relationships while automatically
247 handling interaction effects between predictors (Elith et al., 2008). The four parameters to optimize
248 in these models are the number of trees, interaction depth, learning rate and bag fractions. We varied
249 the parameter settings to find the optimal parameter combination that achieves minimum predictive
250 error. The number of trees was set to 3000, the interaction depth varied from 1 to 7 (at an interval
251 of 1), the learning rate was set to 0.001, 0.01, 0.05 and 0.1, and the bag fraction was set to 0.5, 0.6,
252 0.7 and 0.75. PFT was used as a dummy variable in the boosted regression trees models. This
253 analysis was conducted using the ‘gbm’ function in the ‘gbm’ package (Ridgeway, 2006).

254 We built separate predictive model for each plant functional trait. To select the optimal
255 parameter combination and to evaluate the final model performance for each trait, we calibrated the
256 models 10 times using randomly selected 80% of the data for training the models and validating
257 against the remaining 20% based on cross-validation (Table B3 in Appendix B). The predictive
258 performance was evaluated by regressing the predicted and observed trait values from all repetitions

259 of the cross-validation. The fitting performances of the random forest and boosted regression trees
 260 methods were evaluated using determinate coefficient (R^2), normalized root-mean-square error
 261 (NRMSE) and mean absolute error (MAE). These scores are calculated following Eq. (1), Eq. (2)
 262 and Eq. (3):

$$263 \quad R^2 = 1 - \frac{\sum_{i=1}^n (p_i - o_i)^2}{\sum_{i=1}^n (p_i - \hat{o}_i)^2} \quad (1)$$

$$264 \quad \text{NRMSE} = \frac{\sqrt{\frac{1}{n} \sum_{i=1}^n (p_i - o_i)^2}}{p_{max} - p_{min}} \quad (2)$$

$$265 \quad \text{MAE} = \frac{1}{n} \sum_{i=1}^n |o_i - p_i| \quad (3)$$

266 where p_i and o_i are the predictive values and observed values, respectively; \hat{o}_i is the mean of
 267 the observed values.

268 To quantify the relative importance of each predictor across the two models consistently, we
 269 used the method proposed by Thuiller et al. (2009). This method applies correlation between the
 270 standard predictions fitted with the original data and predictions where the variable under
 271 investigation has been randomly permuted. If the correlation is high, which indicates little
 272 difference between the two predictions, the variable permuted is considered not important for the
 273 model. This step was repeated multiple times for each predictor, and the mean correlation coefficient
 274 over runs was recorded. Then the relative importance of each predictor was quantified as one minus
 275 the Spearman rank correlation coefficient (see Boonman et al., 2020). In addition, we used
 276 generalized additive models to fit the relationships between plant functional traits and the most
 277 important variables using the ‘gam’ function in the ‘mgcv’ package.

278 **2.5 Generation of plant functional trait maps and model performance**

279 The generation of spatial maps of plant functional was performed in three steps. First, we predicted
 280 trait values for each PFT within 1 km grid cell separately. Second, the abundance of individual PFT
 281 within 1 km grid cell was estimated using a land cover map with a spatial resolution of 100 m. Third,
 282 refer to the Eq. (4) that has been widely applied in a community (Garnier et al., 2004), the final trait
 283 value in a given 1 km grid cell was calculated as the sum of the predicted trait values multiplying
 284 by corresponding abundance of each PFT.

$$285 \quad \text{CWM} = \sum_{i=1}^n W_i X_i \quad (4)$$

286 where n is the total number of PFT in a given grid; W_i is the relative abundance of the i th PFT; and
 287 X_i is the predicted trait value of the i th PFT.

288 To reduce the variability of different single-models and to construct a more stable and accurate
 289 model, the ensemble model was further applied to merge the predictions of random forest and
 290 boosted regression trees according to their cross-validated R^2 values. The predictive value of
 291 ensemble model was calculated in a given grid cell as described by Eq. (5) (Marmion et al., 2009).
 292 The model accuracy was calculated by regressing the predictive values of ensemble model against
 293 the observed trait values.

294
$$Pred_EM_t = \frac{\sum_{m=1}^2(pred_{m,t} \times r_{m,t}^2)}{\sum_{m=1}^2 r_{m,t}^2} \quad (5)$$

295 where $Pred_EM_t$ is the predictive values of t trait in the ensemble model; $pred_{m,t}$ is the
 296 predictive values of t trait in m model; $r_{m,t}^2$ is the cross-validated R^2 of t trait in m model.

297 To evaluate the model performance (i.e. the variability in the prediction across models), the
 298 coefficient of variation (CV) was calculated as the difference between the predictions of random
 299 forest and boosted regression trees methods and the ensemble prediction. CV is calculated as
 300 following Eq. (6):

301
$$CV_t = \frac{\sqrt{\sum_{m=1}^2(pred_{m,t} - obs_t)^2 * r_{m,t}^2}}{\sum_{m=1}^2 r_{m,t}^2} \quad (6)$$

302 where $pred_{m,t}$ is the predictive values of t trait in m model; obs_t is the values of t trait in the
 303 ensemble model; $r_{m,t}^2$ is the cross-validated R^2 of t trait in m model.

304 **2.6 Uncertainty assessments**

305 Multivariate environmental similarity surface analysis (MESS) was used to identify the range of the
 306 extrapolated predictor values across the locations in the plant trait dataset (Elith et al., 2010). This
 307 method is often used to evaluate the extent of extrapolation and the applicability domain. If the
 308 values are negative, this indicates that at a given grid cell, at least one predictor variable is outside
 309 the extent of referenced predictor layer. This analysis was conducted using the ‘mess’ function in
 310 the ‘dismo’ package.

311 All analyses were performed in R 4.0.2 (R Core Team, 2020).

312 **3 Results**

313 **3.1 Performances of prediction models**

314 Cross-validation showed that the performance of the predictive models differed greatly among the
 315 plant functional traits (Table 2, Tables C1 and C2 in Appendix C). WD had the best performance in
 316 all three models, with R^2 values of 0.64, 0.68 and 0.67 for random forest, boosted regression trees
 317 and ensemble model, respectively. SLA and LPC had R^2 values greater than 0.45, while LDMC
 318 performed the worst, with R^2 values below 0.25.

319 **Table 2** Results of plant functional traits for cross-validated R², NRMSE and MAE for random
 320 forest, boosted regression trees and ensemble model.

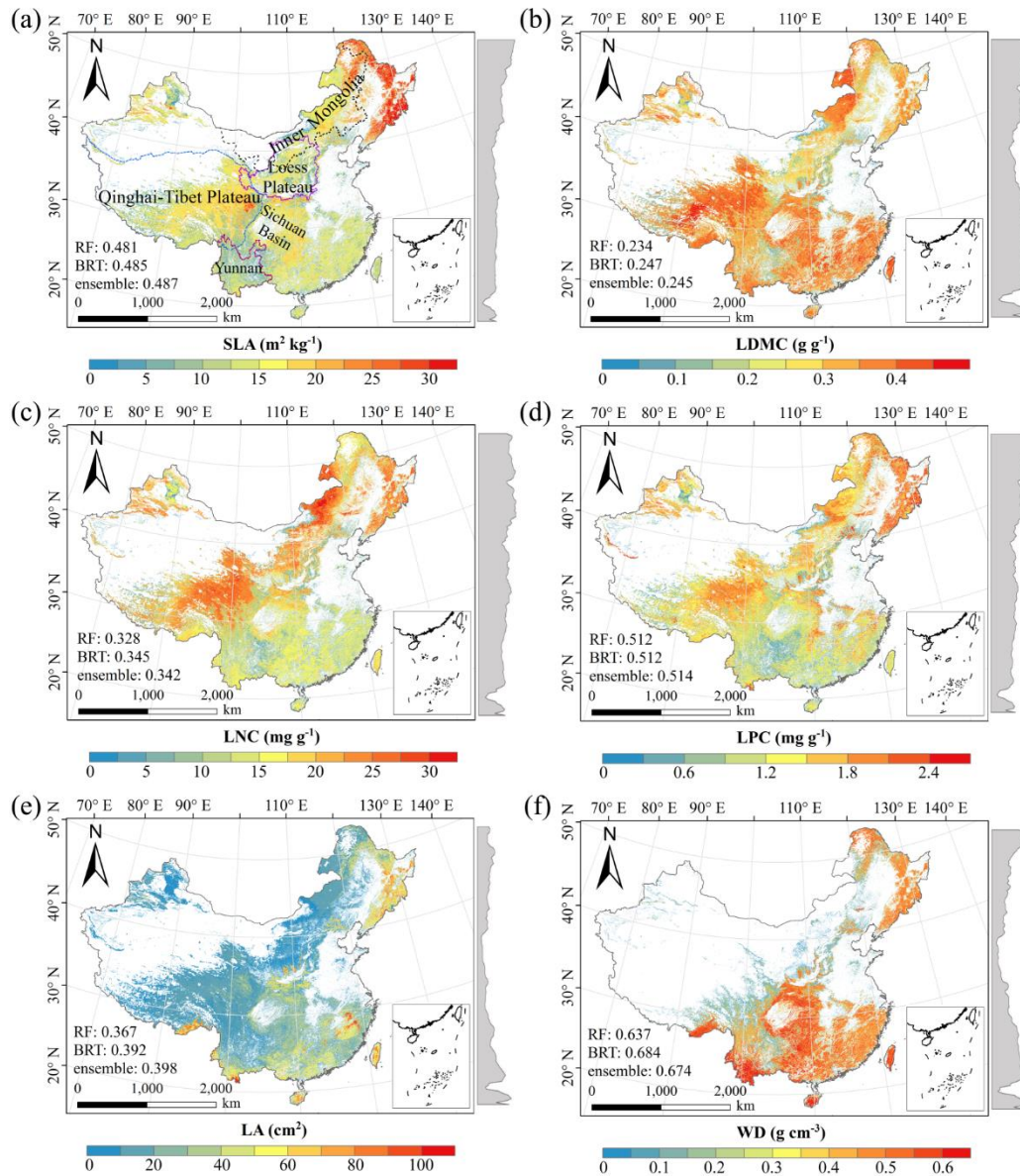
Traits	Random forest			Boosted regression trees			Ensemble model		
	R ²	NRMSE	MAE	R ²	NRMSE	MAE	R ²	NRMSE	MAE
SLA	0.48	0.22	5.10	0.48	0.20	5.08	0.49	0.21	5.07
LDMC	0.23	0.21	0.07	0.28	0.18	0.07	0.24	0.20	0.07
LNC	0.33	0.19	4.92	0.34	0.18	4.85	0.34	0.19	4.85
LPC	0.51	0.24	0.53	0.51	0.22	0.53	0.51	0.27	0.53
LA	0.37	0.45	26.76	0.39	0.51	27.47	0.40	0.58	26.59
WD	0.64	0.20	0.10	0.68	0.13	0.10	0.67	0.17	0.10

321 SLA, specific leaf area (m² kg⁻¹); LDMC, leaf dry matter content (g g⁻¹); LNC, leaf N concentration (mg
 322 g⁻¹); LPC, leaf P concentration (mg g⁻¹); LA, leaf area (cm²); WD, wood density (g cm⁻³); R², determinate
 323 coefficient; NRMSE, normalized root-mean-square error; MAE, mean absolute error.

324 3.2 Spatial patterns of predicted plant functional traits

325 There were relatively consistent spatial patterns for SLA, LNC and LPC, with high values in the
 326 northeastern and northwestern regions and the southeastern Qinghai-Tibet Plateau, and low values
 327 in southwestern China (Figs. 3a, 3c and 3d, Figs. D1 and D2 in Appendix D). SLA and LPC
 328 increased with latitude, while LNC did not vary significantly along the latitudinal gradient. For SLA,
 329 LNC and LPC, the variability was low among random forest, boosted regression trees and ensemble
 330 model, with an overall CV less than 0.3 (Figs. 4a, 4c and 4d). LDMC values were relatively high in
 331 most regions of China, and the low values were mainly located in eastern Yunnan and the Loess
 332 Plateau (Fig. 3b, Figs. D1 and D2 in Appendix D). LA showed high values in the northeastern and
 333 southern regions (except for the Sichuan Basin), and the southeastern Qinghai-Tibet Plateau (Fig.
 334 3e, Figs. D1 and D2 in Appendix D). The strong latitudinal gradient was observed in LA, where
 335 values decreased with latitude.

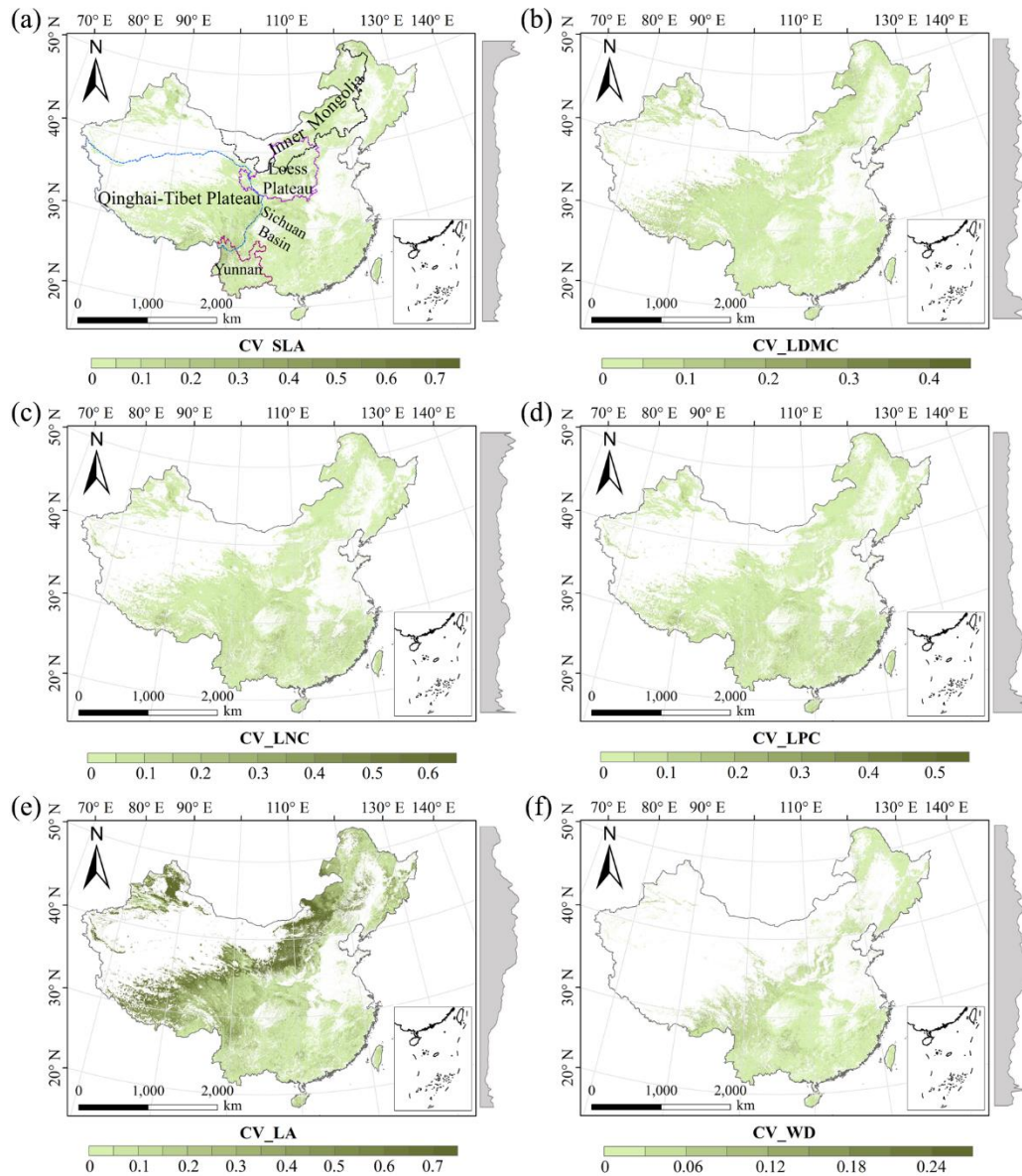
336 The CV values of LPC decreased with latitude, but other traits did not show latitudinal patterns
 337 (Fig. 4). The CV values of LA were relatively high, especially in the northwestern region and the
 338 Inner Mongolia-Loess Plateau region (Fig. 4e). WD had high values in the northeastern and southern
 339 regions (Fig. 2f, Figs. D1 and D2 in Appendix D), while CV values for WD in China were low
 340 throughout China (Fig. 4f).



341

342

Figure 3. Spatial patterns of predicted plant functional traits in China based on the ensemble
 343 model. The grey curves to the right of the maps display trait distribution along with latitude. RF,
 344 random forest; BRT, boosted regression trees; ensemble, ensemble model; SLA, specific leaf area;
 345 LDMC, leaf dry matter content; LNC, leaf N concentration; LPC, leaf P concentration; LA, leaf
 346 area; WD, wood density.



347

348

Figure 4. The variability in plant functional trait predictions among random forest, boosted regression trees and ensemble model. The grey curves to the right of the maps display coefficient of variation along with latitude. SLA, specific leaf area; LDMC, leaf dry matter content; LNC, leaf N concentration; LPC, leaf P concentration; LA, leaf area; WD, wood density.

351

352 **3.3 Relative importance of predictive variables**

353

The dominant factors explaining spatial variation differed greatly among plant functional traits (Table 3). Overall, climate variables were more important for predicting plant functional traits than were soil variables. Temperature variables (i.e., MAT, MDR and TS) showed close relationships with SLA, LDMC, LPC and WD, while precipitation variables (i.e., PS, PEQ, MAP and PDQ) were more important for predicting the spatial patterns of LNC, LPC and LA. RAD was the fourth most dominant factor in predicting the spatial patterns of SLA and WD. Elevation also played an

358

359 important role in the LDMC and LPC predictions. Within soil variables, soil nutrients (i.e., pH and
 360 SAP) showed close associations with SLA and LNC. In addition to the environmental variables,
 361 MTCI emerged as an important predictor for explaining SLA, LDMC and LA. Finally, EVI was the
 362 most important predictor for LA, and MIR in January and May were the primary predictors of WD.
 363 The relationships between plant functional traits and the most important variables were shown in
 364 Figs. E1 and E2 in Appendix E.

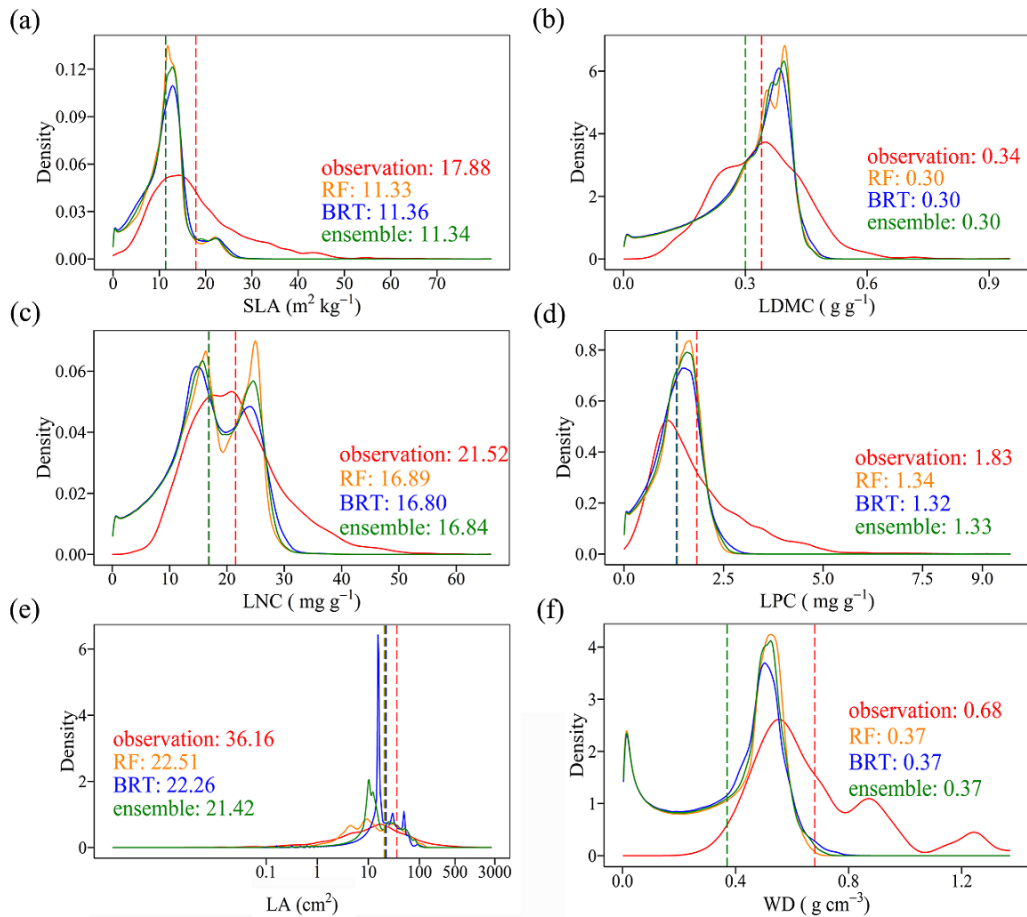
365 **Table 3** List of the eight most important variables for plant functional trait predictions.

Rank	SLA	LDMC	LNC	LPC	LA	WD
1	SAP	MAT	PS	MDR	EVI5	MIR1
2	TS	Elevation	SAP	PDQ	PEQ	TS
3	blue9	MTCI5	pH	Elevation	MTCI9	MIR5
4	RAD	blue8	MDR	MIR8	NIR9	RAD
5	MTCI4	MTCI4	MAP	Tmax	AI	MIR6
6	MTCI6	MTCI6	PEQ	MTCI6	MTCI6	pH
7	Elevation	NIR1	MIR1	MIR7	MAP	red5
8	MTCI7	CEC	Tmax	MIR9	red5	PS

366 SLA, specific leaf area ($\text{m}^2 \text{kg}^{-1}$); LDMC, leaf dry matter content (g g^{-1}); LNC, leaf N concentration (mg
 367 g^{-1}); LPC, leaf P concentration (mg g^{-1}); LA, leaf area (cm^2); WD, wood density (g cm^{-3}); SAP, soil
 368 available P; TS, temperature seasonality; blue, blue reflectance; RAD, solar radiation; MTCI, MERIS
 369 terrestrial chlorophyll index; MAT, mean annual temperature; NIR, near-infrared reflectance; CEC,
 370 cation exchange capacity; PS, precipitation seasonality; MDR, mean diurnal range; MAP, mean annual
 371 precipitation; PEQ, precipitation of wettest quarter of a year; MIR, middle infrared reflectance; Tmax,
 372 max temperature of warmest month of a year; PDQ, precipitation of driest quarter of a year; EVI,
 373 enhanced vegetation index; AI, aridity index; red, red reflectance.

374 **3.4 Model performance**

375 The distributions of the predictive trait values based on random forest, boosted regression trees, and
 376 ensemble model were consistent with the original trait observations, especially the peak values (Fig.
 377 5). The mean values of trait observations were relatively higher than those of the predictive values.



378

379

Figure 5. Comparison of trait distribution between observations and predictive values in each of the different models. Each panel depicts the distribution of observations in solid red, of the random forest (RF) model in yellow, of the boosted regression trees (BRT) model in blue, and of the ensemble model in green. The dashed vertical lines indicate mean values. SLA, specific leaf area; LDMC, leaf dry matter content; LNC, leaf N concentration; LPC, leaf P concentration; LA, leaf area; WD, wood density.

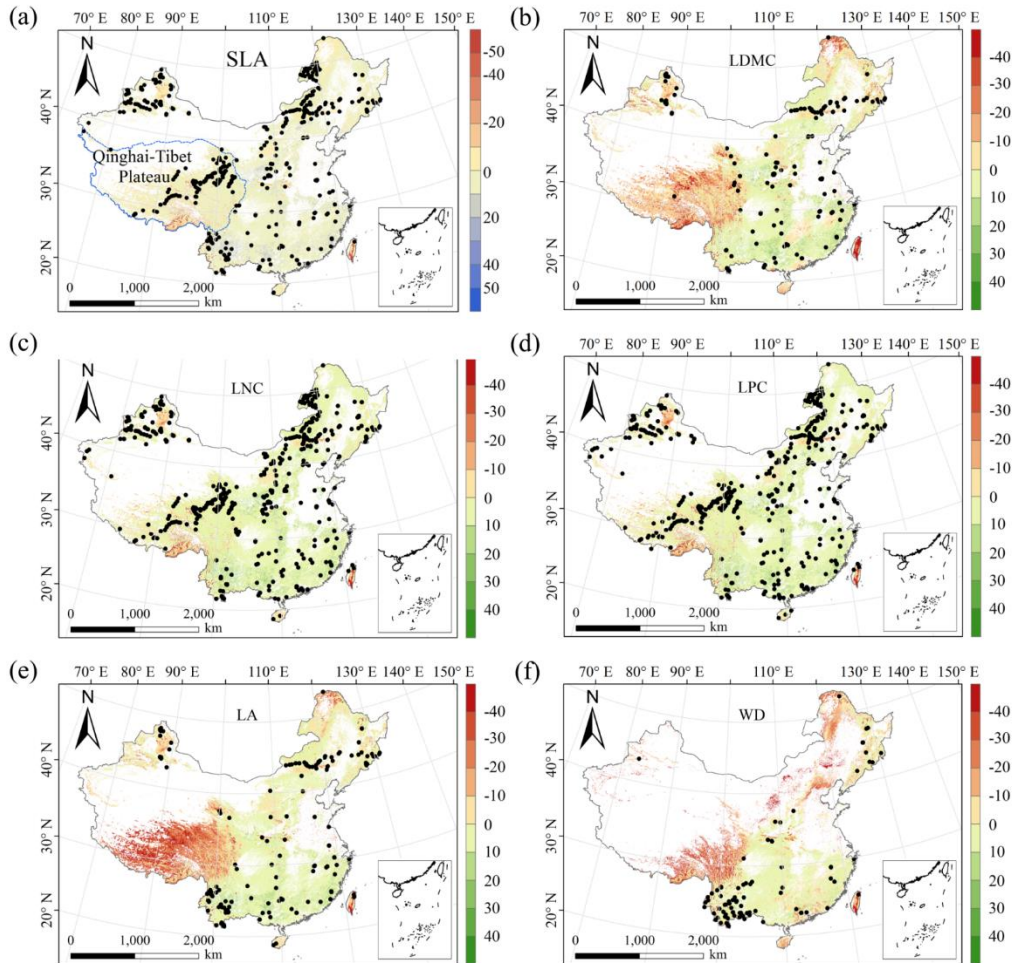
385

3.5 Uncertainty assessments

386

The MESS values of all plant functional traits were positive in most regions, indicating a wide applicability domain of our models (Fig. 6). Nevertheless, trait predictions should be interpreted carefully for northeastern China and the Qinghai-Tibet Plateau due to the sparse samplings in these regions.

389



390

391 **Figure 6.** Multivariate environmental similarity surface (MESS) assessments for the six plant
 392 functional traits. The black dots represented the locations of trait observations. More intense shades
 393 indicate greater similarity (blue) or difference (red) in environmental conditions of the location
 394 compared to the predictive factors covered by the training dataset. SLA, specific leaf area; LDMC,
 395 leaf dry matter content; LNC, leaf N concentration; LPC, leaf P concentration; LA, leaf area; WD,
 396 wood density.

397 **4 Discussion**

398 **4.1 Comparison with previous work**

399 Our study predicted the spatial patterns of six key plant functional traits across China using machine
 400 learning methods and identified the applicability domain of the models. WD had the highest
 401 precision with a R^2 of 0.66, which was higher than the global WD prediction (Boonman et al., 2020).
 402 This improvement in precision may be attributed to the large number and dense occurrence of
 403 sample sites as well as the inclusion of vegetation indices in our study. In addition, SLA and LPC
 404 also showed good accuracy with R^2 values of 0.50, which was higher than that of Boonman et al.
 405 (2020) and consistent with that of Moreno-Martínez et al. (2018). However, LNC and LA showed

406 relatively poor performance, which may be related to the reason that these two traits were more
407 influenced by phylogeny than environmental variables (Yang et al., 2017; An et al., 2021).

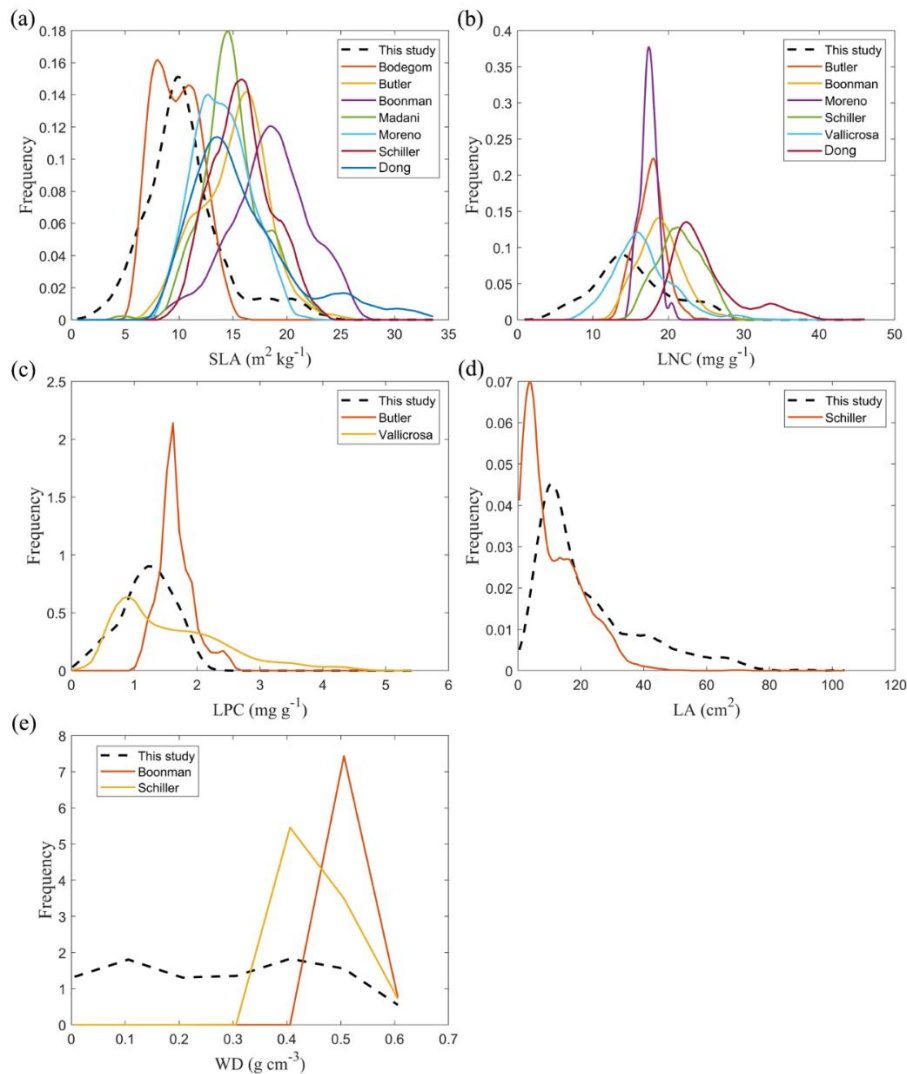
408 The frequency distribution of plant functional traits in China differed between our study and
409 previous studies (Fig. 7, Fig. F1, Table F1 in Appendix F). Given that the spatial resolution of trait
410 maps in most previous studies is 0.5° (except for Moreno-Martínez et al. (2018) and Vallicrosa et
411 al. (2022)), we resampled the data products of previous studies and our study to 0.5° spatial
412 resolution. The distribution in our study contained more predictions at lower values of SLA, LNC
413 and LPC and was broader than those for SLA and LNC in previous global studies. However, the
414 distribution of LNC in our study was consistent with that in Vallicrosa et al. (2022) at the 1 km
415 spatial resolution (Fig. F1 in Appendix F). LA in our study contained more predictions at higher
416 values and was also broader than those in previous global studies. WD did not show the lower and
417 higher predictive values, however, the WD values in the studies of Boonman et al. (2020) and
418 Schiller et al. (2021) had more predictions at higher values and no lower values ($< 0.3 \text{ g cm}^{-3}$). Our
419 predicted values of SLA showed the highest spatial correlation with those of Dong et al. (2023), and
420 LNC showed the strongest spatial correlation with those of Butler et al. (2017) (Table 5). LA and
421 WD showed the best spatial correlation with those of Schiller et al. (2021), but LPC showed
422 relatively weak spatial correlation with those of published studies.

423 In addition, we compared our results to the other studies focused on China. Yang et al. (2016)
424 predicted the spatial distribution of leaf mass per area (1/SLA) and LNC based on trait-environment
425 relationships in China and had an R^2 of 0.13-0.16. The lower predictive precision may be because
426 Yang et al. (2016) only used MAT, MAP and RAD as predictors in estimating the spatial patterns of
427 leaf mass per area and LNC, which likely led to poor performance and low heterogeneity. These
428 results also demonstrated the advantage of our methods in mapping the spatial patterns of plant
429 functional traits at a regional scale.

430 **Table 5** Spatial correlations for SLA, LNC, LPC, LA and WD between this study and other
 431 previous trait maps, labelled by the first author of the corresponding publication (see Table F1 in
 432 Appendix F for citations)

Spatial correlation	Dong	Vallicrosa	Schiller	Boonman	Moreno	Madani	Butler	Bodegom
SLA	0.398		-0.082	0.327	0.242	0.136	-0.042	0.319
LNC	0.156	0.359	0.229	0.252			0.394	
LPC		0.136					0.057	
LA			0.514					
WD			0.647	0.107				

433 The spatial correlation of LDMC between our study and previous study was not included, as the LDMC
 434 maps were not available. SLA, specific leaf area ($\text{m}^2 \text{kg}^{-1}$); LNC, leaf N concentration (mg g^{-1}); LPC,
 435 leaf P concentration (mg g^{-1}); LA, leaf area (cm^2); WD, wood density (g cm^{-3}).



436 **Figure 7.** Frequency distributions of plant functional traits in our study (“This study”, dashed
 437 black lines) and other trait maps, identified by the first author of the corresponding publication (see
 438 Table F1 for citations). SLA, specific leaf area ($\text{m}^2 \text{kg}^{-1}$); LNC, leaf N concentration (mg g^{-1}); LPC,
 439 leaf P concentration (mg g^{-1}); LA, leaf area (cm^2); WD, wood density (g cm^{-3}).

441 **4.2 Spatial patterns of plant functional traits in China**

442 Our study revealed the spatial patterns of different plant functional traits across China, and the
443 variability among the two machine learning methods was relatively low. We compared the spatial
444 differences of trait maps between our study and previous studies at the global scale (Figs. F2-F6 in
445 Appendix F). For example, our study showed high SLA values in the southeastern Qinghai-Tibet
446 Plateau, which concurred with the global study of Boonman et al. (2020). The spatial difference of
447 SLA between our study and Bodegom et al. (2014) was relatively low, and the predictive values in
448 most regions were slightly lower in our study than those in Bodegom et al. (2014). The spatial
449 pattern of difference in SLA between our study and Moreno et al. (2018), Bulter et al. (2017) and
450 Bodegom et al. (2020) was consistent, and the values were higher in northeastern China and
451 southwestern Qinghai-Tibet Plateau in our study than those studies. Our study showed higher LNC
452 values in the northern Inner Mongolia-the Loess Plateau-the eastern Qinghai-Tibet Plateau and
453 northwestern China than those studies at the global studies (Butler et al., 2017; Moreno-Martínez
454 et al., 2018; Boonman et al., 2020; Vallicrosa et al., 2022; Dong et al., 2023), reflecting the consistent
455 spatial pattern among these studies. However, Yang et al. (2016) predicted high LNC values in
456 northeastern and northwestern China, northern Inner Mongolia and the entire Qinghai-Tibet Plateau,
457 and SLA and LNC had low heterogeneity overall. The discrepancy with Yang et al. (2016) may be
458 attributed to spatial extrapolation based on trait-climate relationships with a low predictive precision.
459 There was no consistent spatial pattern in LPC between our study and previous studies. Consistent
460 with the global pattern (Wright et al., 2017), LA was larger in southern regions than in northern
461 regions and showed a decreasing trend with latitude. In addition, LA and WD values in our study
462 were lower in most regions than those ones at the global scale. These discrepancies between our
463 study and previous studies at the global scale may be related to three reasons. First, there is bias in
464 the available in-situ field measurement data from China in these global studies, with large gaps in
465 western China for SLA and no data in China for WD (Boonman et al., 2020). Second, some trait-
466 environment relationships may be scale dependent (Bruehlheide et al., 2018), and these studies we
467 compared are from the global scale due to the trait maps in China are not available. Third, the
468 methods used for trait mapping were different among studies, including eco-evolutionary optimality
469 models (Dong et al., 2023), Convolutional Neural Networks based on RGB photographs (Schiller
470 et al., 2021), machine learning algorithms (Vallicrosa et al., 2022; Boonman et al., 2020) and
471 multiple regression analysis (Bodegom et al., 2014).

472 Moreover, our study also identified the applicability domain of our models for predicting the
473 spatial patterns of plant functional traits across China. Five leaf traits and WD appeared to have poor
474 applicability in northeastern China and the Qinghai-Tibet Plateau, primarily due to sparse samplings.
475 Future studies predicting plant functional traits across a large scale through remote sensing
476 observations or other supplementary data will be needed to re-evaluate our results.

477 **4.3 The role of predictive variables**

478 Our study indicates that environmental variables are important for predicting the spatial patterns of
479 plant functional traits, especially climate variables. Temperature variables were primary predictors
480 for SLA, LDMC, LPC and WD. The relationships between leaf traits and temperature have been
481 widely discussed in global and regional studies (Reich and Oleksyn, 2004; Bruelheide et al., 2018).
482 The positive linkage between WD and temperature may be driven by changes in the viscosity of
483 water. Plants can adapt to the low water viscosity at high temperatures by reducing the diameter and
484 density of their vessels and by thickening cell walls (Roderick and Berry, 2002; Thomas et al., 2004).
485 Precipitation variables were important predictors for leaf nutrient traits and LA. For example,
486 precipitation of wettest quarter of a year was the factor that most influenced LA variation, which
487 has been confirmed by a previous study (An et al., 2021). A smaller LA could be an adaptive strategy
488 to decrease water loss via reducing the surface area for transpiration under dry environmental
489 conditions (Du et al., 2019). Although the effects of soil on trait predictions were relatively weak,
490 we found that SAP and pH played key roles in SLA and LNC predictions. These results were similar
491 with the previous studies that reported that soil pH was an important driver of trait variation at the
492 global scale and in tundra regions (Maire et al., 2015; Kemppinen et al., 2021). Additionally, from
493 the perspective of cost-efficient theory, the strong effects of SAP reflected that high SLA may be an
494 adaptation for facilitating soil exploration more efficiently in fertile soils (Freschet et al., 2010).

495 Vegetation indices have recently been proposed as important predictors of spatial patterns of
496 plant functional traits (Loozen et al., 2018). Our results corroborate these findings and further
497 suggest that EVI, MTCI and MIR reflectance are important predictors in models. Here, the
498 underlying mechanisms between vegetation indices and plant functional traits are not further
499 discussed due to their complexity and uncertainty. However, our results indicated that vegetation
500 indices and NIR reflectance are not key predictors of LNC estimation, which contrasts the findings
501 from global and regional studies (Wang et al., 2016; Loozen et al., 2018; Moreno-Martínez et al.,
502 2018). This may be related to the multitude of factors that influence the relationship between LNC
503 and vegetation indices and NIR reflectance, such as forest type and canopy structure (Dahlin et al.,
504 2013).

505 **4.4 Uncertainties**

506 Although our study mapped the spatial patterns of key functional traits of seed plants in China
507 through large-scale field investigations and compared the predictions with previous studies
508 performed at global and regional scales, there persists some uncertainties in the interpretation of
509 these results. First, the predictive ability of models was relatively worse for certain traits, especially
510 LDMC. Beyond the environmental effects, the variation in plant functional traits is also regulated
511 by phylogenetic structure among plant species (e.g., family, order and phylogenetic clade) (Li et al.,
512 2017). Consequently, incorporating the phylogenetic information will be a promising avenue for
513 further improving the accuracy of spatial predictions of plant functional traits (Butler et al., 2017).

514 A second potential issue is sampling bias; there were major spatial gaps in field investigation in both
515 the northeastern China and the Qinghai-Tibet Plateau. Due to the lack of measurements for small
516 shrubs and low vegetation, WD data is mainly confined to eastern forests, and the overall quantity
517 of WD data was much lower than that of leaf traits, even in the TRY database. The environmental
518 information of sampling sites was not always obtained from original literature, thus using the public
519 environmental products is a common resolution in large-scale plant trait studies (Boonman et al.,
520 2020; Vallicrosa et al., 2022). Such mismatch between in-situ trait measurements and predictors
521 should be resolved in further work. Finally, additional key challenges in data availability must be
522 resolved to scale up from the species to the community levels, in particular with data surrounding
523 species co-occurrence and their relative cover or abundance in ecological communities (He et al.,
524 2023). Global biodiversity data (e.g., sPlot and Global Biodiversity Information Agency databases)
525 that contains information on species occurrence or the proportion of species in a community has the
526 potential for enabling the calculation of community-weighted trait values and the re-evaluation of
527 our results in future work (Telenius, 2011; Bruelheide et al., 2019). The lack of consistent time
528 period and spatial resolution of predictors due to limitation of data availability is another key
529 challenges in the spatial mapping of plant functional traits. In addition, although WorldClim version
530 2.1 product has high spatial resolution and includes various aspects of climatic parameters, there
531 exists certain limitation and uncertainty in predicting trait maps. Therefore, integrating satellite
532 remote sensing monitoring methods with in-situ trait data collection can also provide an effective
533 way to estimate and assess the species diversity at a large scale (Cavender-Bares et al., 2022).

534 **4.5 Potential applications**

535 Maps of these key functional traits of seed plants highlighted large-scale variability in space, which
536 will significantly advance ecological analyses and future interdisciplinary research. First, using the
537 spatially continuous trait maps, one can optimize and develop trait-flexible vegetation models,
538 which allows for the exploration of the community assembly rules based on how plants with
539 different trait combinations perform under a given set of environmental conditions (Berzaghi et al.,
540 2020). When trait-flexible vegetation models are available, incorporating trait maps into models
541 will bridge the gap for vegetation classifications and predictions of vegetation distribution under
542 global change, which is not feasible in conventional vegetation models (Van Bodegom et al., 2012;
543 Yang et al., 2019). Second, the assessments of China's terrestrial ecosystem carbon sink have had
544 large uncertainties so far (Piao et al., 2022), but the spatial continuous trait maps will provide an
545 effective way to link ecosystem characteristics to ecosystem carbon sink estimates in China (Madani
546 et al., 2018; Šimová et al., 2019). These analyses will help shed light on the mechanisms underlying
547 plant functional traits and terrestrial ecosystem carbon storage at a large scale.

548 **5 Data availability**

549 The original plant functional trait data collected in this study that were used for machine learning

550 models (named by Data file used for machine learning models.csv) and final maps of plant
551 functional traits in terrestrial ecosystems in a GeoTIFF format across China (named by plant
552 functional trait category) are now available for the private link
553 <https://figshare.com/s/c527c12d310cb8156ed2> (An et al., 2023). Once the article is accepted, we
554 will publicly publish these maps at the figshare website.

555 **6 Conclusions**

556 We generated a set of spatial continuous trait maps at a 1-km spatial resolution using machine
557 learning methods in combination with field measurements, environmental variables and vegetation
558 indices. Models for leaf traits (except for LDMC) and WD showed good accuracy and robustness,
559 whereas models of LDMC had relatively poor precision and robustness. Temperature variables were
560 the most important predictors for leaf traits (except for LA) and WD, and precipitation variables
561 were the most important predictors for leaf nutrient traits and LA. We caution that plant functional
562 trait predictions should be interpreted carefully for northeastern China and the Qinghai-Tibet Plateau.
563 The spatial continuous trait maps generated in our study are complementary to current terrestrial in-
564 situ observations and offer new avenues for predicting large-scale changes in vegetation and
565 ecosystem function under climate scenarios in China.

566

567 **Appendix A Data collection from literature**

- 568 An H. and Shanguan Z. P. Photosynthetic characteristics of dominant plant species at different succession stages of
569 vegetation on Loess Plateau. *Chinese Journal of Applied Ecology*, 2007, 18, 1175-1180.
- 570 Bai K. D., Jiang D. B., Wan C. X. Photosynthesis-nitrogen relationship in evergreen and deciduous tree species at
571 different altitudes on Mao'er Mountain, Guangxi. *Acta Ecologica Sinica*, 2013, 33, 4930-4938.
- 572 Bai W. J., Zheng F. L., Dong L. L., et al. Leaf traits of species in different habits in the water-wind erosion region of
573 the Loess Plateau. *Acta Ecologica Sinica*, 2010, 30, 2529-2540.
- 574 Chai Y. F., Shang H. L., Zhang X. F., et al. Ecological variations of woody species along an altitudinal gradient in
575 the Qinling Mountains of Central China: area-based versus mass-based expression of leaf traits. *Journal of*
576 *Forestry Research*, 2021, 32, 599-608.
- 577 Chang Y. N., Zhong Q. L., Cheng D. L., et al. Stoichiometric characteristics of C, N, P and their distribution pattern
578 in plants of *Castanopsis carlesii* natural forest in Youxi. *Journal of Plant Resources and Environment*, 2013, 22,
579 1-10.
- 580 Chen F. Y., Luo T. X., Zhang L., et al. Comparison of leaf construction cost in dominant tree species of the evergreen
581 broadleaved forest in Jiulian Mountain, Jiangxi Province. *Acta Ecologica Sinica*, 2006, 26, 2485-2493.
- 582 Chen H. Y., Huang Y. M., He K. J., et al. Temporal intraspecific trait variability drives responses of functional
583 diversity to interannual aridity variation in grasslands. *Ecology and Evolution*, 2018, 9, 5731-5742.
- 584 Chen L. X., Xiang W. H., Wu H. L., et al. Tree growth traits and social status affect the wood density of pioneer
585 species in secondary subtropical forest. *Ecology and Evolution*, 2017, 7, 5366-5377.
- 586 Chen L., Yang X. G., Song N. P., et al. Leaf water uptake strategy of plants in the arid-semiarid region of Ningxia.
587 *Journal of Zhejiang University*, 2013, 39, 565-574.
- 588 Chen Y. H., Han W. X., Tang L. Y., et al. Leaf nitrogen and phosphorus concentrations of woody plants differ in

589 responses to climate, soil and plant growth form. *Ecography*, 2011, 36, 178-184.

590 Cheng J. H., Chu P. F., Chen D. M., et al. Functional correlations between specific leaf area and specific root length
591 along a regional environmental gradient in Inner Mongolia grasslands. *Functional Ecology*, 2016, 30, 985-997.

592 Cheng W., Yu C. H., Xiong K. N., et al. Leaf functional traits of dominant species in karst plateau-canyon areas.
593 *Guihaia*, 2019, 39, 1039-1049.

594 Dong H. and Shekhar R. B. Negative relationship between interspecies spatial association and trait dissimilarity.
595 *Oikos*, 2019, 128, 659-667.

596 Dong T. F., Feng Y. L., Lei Y. B., et al. Comparison on leaf functional traits of main dominant woody species in wet
597 and dry habitats. *Chinese Journal of Ecology*, 2012, 31, 1043-1049.

598 Du H. D. Ecological responses of foliar anatomical structural & physiological characteristics of dominant plants at
599 different site conditions in north Shaanxi Loss Plateau. 2010, Graduation Thesis.

600 Fan Z. X., Zhang S. B., Hao G. Y., et al. Hydraulic conductivity traits predict growth rates and adult stature of 40
601 Asian tropical tree species better than wood density. *Journal of Ecology*, 2012, 100, 732-741.

602 Feng J. B., Fan S. X., Hou Y. F., et al. Interspecific and intraspecific variation of leaf function traits of herbaceous
603 plants in a forest-steppe zone, Hebei Province, China. *Journal of Northeast Forestry University*, 2021, 49, 23-
604 28.

605 Feng Q. H. The study on the response of foliar $\delta^{13}C$ of different life from plants to altitude in subalpine area of
606 Western Sichuan, China. 2011, Graduation Thesis.

607 Fu P. L., Zhu S. D., Zhang J. L., et al. The contrasting leaf functional traits between a karst forest and a nearby non-
608 karst forest in south-west China. *Functional Plant Biology*, 2019, 46, 907-915.

609 Gao S. P., Li J. X., Xu M. C., et al. Leaf N and P stoichiometry of common species in successional stages of the
610 evergreen broad-leaved forest in Tiantong National Forest Park, Zhejiang Province, China. *Acta Ecologica
611 Sinica*, 2007, 27, 947-952.

612 Geekiyana N., Goodale, U. M., Cao, K. F., et al. Leaf trait variations associated with habitat affinity of tropical
613 karst tree species. *Ecology and Evolution*, 2017, 8, 286-295.

614 Geng Y., Ma W. H., Wang L., et al. Linking above- and belowground traits to soil and climate variables: an integrated
615 database on China's grassland species. *Ecology*, 2017, 98, 1471.

616 Guo F. C. The photosynthetic characteristics of precious broad-leaved tree species in south subtropics and their
617 relationship with leaf functional traits. 2015, Graduation Thesis.

618 Guo W. J. Exploring the relationship between arbuscular mycorrhizal fungi and plant based on phylogeny and plant
619 traits. 2015, Graduation Thesis.

620 Hau C. H. Tree seed predation on degraded hillsides in Hong Kong. *Forest Ecology & Management*. 1997, 99, 215-
621 221.

622 He J. S., Wang Z. H., Wang X. P., et al. A test of the generality of leaf trait relationships on the Tibetan Plateau. *New
623 Phytologist*, 2006, 170, 835-848.

624 He P. C., Wright I. J., Zhu S. D., et al. Leaf mechanical strength and photosynthetic capacity vary independently
625 across 57 subtropical forest species with contrasting light requirements. *New Phytologist*, 2019, 223, 607-618.

626 He Y. T. Studies on physioecological traits of 30 plant species in the Subalpine Meadow of the Qinling Mountains.
627 2007, Graduation Thesis.

628 Hou M. M. Adaptive evolution of some species from sedges (*Carex Cyperaceae*) based on phylogeny and leaf
629 functional traits to habitat in the Poyang Lake Area. 2017, Graduation Thesis.

630 Hou Y., Liu M. X., Sun H. R., et al. Response of plant leaf traits to microhabitat change in a subalpine meadow on
631 the eastern edge of Qinghai-Tibetan Plateau, China. *Chinese Journal of Applied Ecology*, 2017, 28, 71-79.

632 Hu Z. Z., Michaletz S. T., Johnson D. J., et al. Traits drive global wood decomposition rates more than climate.

633 Global Change Biology, 2018, 24, 5259-5269.

634 Hua L., He P., Goldstein G., et al. Linking vein properties to leaf biomechanics across 58 woody species from a
635 subtropical forest. *Plant Biology*, 2019, 22, 212-220.

636 Huang J. J. and Wang X. H. Leaf nutrient and structural characteristics of 32 evergreen broad-leaved species. *Journal*
637 *of East China Normal University (Natural Science)*, 2003, 1, 92-97.

638 Huang Y. L. The research about the turnover patterns and moisture adaptation mechanism of major species on the
639 South-North-facing slope. 2012, Graduation Thesis.

640 Iida Y., Kohyama T. S., Swenson N. G., et al. Linking functional traits and demographic rates in a subtropical tree
641 community: the importance of size dependency. *Journal of Ecology*, 2014, 102, 641-650.

642 Jia Q. Q. Functional traits of fine roots and their relationship with leaf traits of 50 major species in a subtropical
643 forest in Gutianshan. 2011, Graduation Thesis.

644 Jiang Y., Chen X., Ma J., et al., Interspecific and intraspecific variation in functional traits of subtropical evergreen
645 and deciduous broadleaved mixed forests in karst topography, Guilin, Southwest China. *Tropical Conservation*
646 *Science*, 2016, 9.

647 Jin Y., Wang C. K., Zhou Z. H., et al. Co-ordinated performance of leaf hydraulics and economics in 10 Chinese
648 temperate tree species. *Functional Plant Biology*, 2016, 43, 1082-1090.

649 Jing G. H. Responses of grassland community structure and functions to management practices on the semi-arid area
650 of Loess Plateau. 2017, Graduation Thesis.

651 Kang M. Spatial distribution pattern and its causes of woody plant functional traits in Tiantong region, Zhejiang
652 Province. 2012, Graduation Thesis.

653 Krober W., Li Y., Hardtle W., et al. Early subtropical forest growth is driven by community mean trait values and
654 functional diversity rather than the abiotic environment. *Ecology and Evolution*, 2015, 5, 3541-3556.

655 Krober W., Bohnke M., Welk E., et al. Leaf trait-environment relationships in a subtropical broadleaved forest in
656 south-east China. *PloS One*, 2012, 7, e35742.

657 Krober W., Zhang, S. R. Ehmig, M., et al. Linking xylem hydraulic conductivity and vulnerability to the leaf
658 economics spectrum-a cross-species study. *PloS One*, 2014, e109211.

659 Li F. Comparison of functional traits in semi-humid evergreen broad-leaved in Western Hill of Kunming. 2011,
660 Graduation Thesis.

661 Li K. and Xiang W. H. Comparison of specific leaf area, SPAD value and seed mass among subtropical tree species
662 in hilly area of Central Hunan, China. *Journal of Central South University of Forestry & Technology*, 2011, 31,
663 213-218.

664 Li L., McCormack M. L., Ma C.G., et al. Leaf economics and hydraulic traits are decoupled in five species-rich
665 tropical-subtropical forests. *Ecology Letters*, 2015, 18, 899-906.

666 Li Q. Leaf functional traits and their relationships with environmental factors in Beishan Mountain of Jinhua,
667 Zhejiang Province. 2020, Graduation Thesis.

668 Li S. J., Su P. X., Zhang H. N., et al. Characteristics and relationships of foliar water and leaf functional traits of
669 desert plants. *Plant Physiology Journal*, 2013, 49, 153-160.

670 Li W. H., Xu F. W., Zheng S. X., et al. Patterns and thresholds of grazing-induced changes in community structure
671 and ecosystem functioning: species-level responses and the critical role of species traits. *Journal of Applied*
672 *Ecology*, 2017, 54, 963-975.

673 Li W. Q., Xu Q., Li J., et al. Quantification of ecotone width of returned forest land from farmland based on specific
674 leaf area. *Journal of West China Forestry Science*, 2017, 46, 117-121.

675 Li X. F., Pei K. Q., Kery M., et al. Decomposing functional trait associations in a Chinese subtropical forest. *PloS*
676 *One*, 2017, 12, e0175727.

677 Li X. F., Schmid B., Wang F., et al. Net assimilation rate determines the growth rates of 14 species of subtropical
678 forest trees. *PLoS One*, 2016, 11, e0150644.

679 Li X. L., Li X. H., Jiang D. M., et al. Leaf morphological characters of 22 compositae herbaceous species in Horqin
680 sandy land. *Chinese Journal of Ecology*, 2005, 24, 1397-1401.

681 Li Y. H., Luo T. X., Lu Q., et al. Comparisons of leaf traits among 17 major plant species in Shazhuyu Sand Control
682 Experimental Station of Qinghai Province. *Acta Ecologica Sinica*, 2005, 25, 994-999.

683 Li Y. L., Meng Q. T., Zhao X. Y., et al. Relationships of fresh leaf traits and leaf litter decomposition in Kerqin Sandy
684 Land. *Acta Ecologica Sinica*, 2008, 28, 2486-2494.

685 Li Y., Yao J., Yang S., et al. Trait differences research on leaf function of Liaodong oak forest main species in
686 Dongling mountain. *Guangdong Agricultural Sciences*, 2012, 23, 159-162, 171.

687 Liang X. Y., Ye Q., Liu H., et al. Wood density predicts mortality threshold for diverse trees. *New Phytologist*, 2021,
688 229, 3053-3057.

689 Li, R., Zhu, S., Chen, H. Y. H., et al. Are functional traits a good predictor of global change impacts on tree species
690 abundance dynamics in a subtropical forest? *Ecology Letters*, 2015, 18, 1181-1189.

691 Li Y. Y., Shi H., Shao M. A. Cavitation resistance of dominant trees and shrubs in Loess hilly region and their
692 relationship with xylem structure. *Journal of Beijing Forestry University*, 2010, 32, 8-13.

693 Lin G. G., Guo, D. L., Li, L., et al. Contrasting effects of ectomycorrhizal and arbuscular mycorrhizal tropical tree
694 species on soil nitrogen cycling: the potential mechanisms and corresponding adaptive strategies. *Oikos*, 2018,
695 127, 518-530.

696 Liu C. H. and Li Y. Y. Relationship between leaf traits and PV curve parameters in the typical deciduous woody
697 plants occurring in Southern Huanglong Mountain. *Journal of Northwest Forestry University*, 2013, 28, 1-5.

698 Liu G. F., Freschet G. T., Pan X., et al. Coordinated variation in leaf and root traits across multiple spatial scales in
699 Chinese semi-arid and arid ecosystems. *New Phytologist*, 2010, 188, 543-553.

700 Liu G. F., Wang L., Jiang L., et al. Specific leaf area predicts dryland litter decomposition via two mechanisms.
701 *Journal of Ecology*, 2017, 106, 218-229.

702 Liu J. H., Zeng D. H. and Don K. L. Leaf traits and their interrelationships of main plant species in southeast Horqin
703 sandy land. *Chinese Journal of Ecology*, 2006, 25, 921-925.

704 Liu J. X., Chen J., Jiang M. X., et al. Leaf traits and persistence of relict and endangered tree species in a rare plant
705 community. *Functional Plant Biology*, 2012, 39, 512-518.

706 Liu L. H. The traits and adaptive strategies of main herbaceous plants and lianas on micro-topographical units in
707 Huangcangyu reserves of Anhui Province. 2012, Graduation Thesis.

708 Liu M. C., Kong D. L., Lu X. R., et al. Higher photosynthesis, nutrient- and energy-use efficiencies contribute to
709 invasiveness of exotic plants in a nutrient poor habitat in northeast China. *Physiologia Plantarum*, 2017, 160,
710 373-382.

711 Liu R. H., Bai J. L., Bao H., et al. Variation and correlation in functional traits of main woody plants in the
712 *Cyclobalanopsis glauca* community in the karst hills of Guilin, southwest China. *Chinese Journal of Plant
713 Ecology*, 2020, 44, 828-841.

714 Liu W. D., Su J. R., Li S. F., et al. Stoichiometry study of C, N and P in plant and soil at different successional stages
715 of monsoon evergreen broad-leaved forest in Pu'er, Yunnan Province. *Acta Ecologica Sinica*, 2010, 30, 6581-
716 6590.

717 Liu X. C., Jia H. B., Wang Q. Y. Genetic variation and correlation in wood properties of *Betula platyphlla* in natural
718 Stands. *Journal of Northeast Forestry University*, 2018, 36, 8-10.

719 Liu Y. Y. Spatial distribution and habitat associations of trees in a typical mixed broad-leaved Korean pine (*Pinus
720 koraiensis*) forest. 2014, Graduation Thesis.

721 Luo Y. H., Cadotte M. W., Burgess K. S., et al. Greater than the sum of the parts: how the species composition in
722 different forest strata influence ecosystem function. *Ecology Letters*, 2019, 22, 1449-1461.

723 Lv J. Z., Miao Y. M., Zhang H. F., et al. Comparisons of leaf traits among different functional types of plant from
724 Huoshan Mountain in the Shanxi Province. *Plant Science Journal*, 2010, 28, 460-465.

725 Ma J., Wu L. F., Wei X., et al. Habitat adaptation of two dominant tree species in a subtropical monsoon forest: leaf
726 functional traits and hydraulic properties. *Guihaia*, 2015, 35, 261-268.

727 Mo J. M., Zhang D. Q., Huang Z. L., et al. Distribution pattern of nutrient elements in plants of Dinghushan Lower
728 Subtropical Evergreen Broad-Leaved Forest. *Journal of Tropical and Subtropical Botany*, 2000, 8, 198-206.

729 Niu C. Y., Meinzer F. C. and Hao G. Y. Divergence in strategies for coping with winter embolism among co-occurring
730 temperate tree species: the role of positive xylem pressure, wood type and tree stature. *Functional Ecology*,
731 2017, 31, 1550-1560.

732 Niu D. C., Li Q., Jiang S. G., et al. Seasonal variations of leaf C:N:P stoichiometry of six shrubs in desert of China's
733 Alxa Plateau. *Chinese Journal of Plant Ecology*, 2013, 37, 317-325.

734 Niu K. C., He J. S. and Lechowicz M. J. Grazing-induced shifts in community functional composition and soil
735 nutrient availability in Tibetan alpine meadows. *Journal of Applied Ecology*, 2016, 53, 1554-1564.

736 Niu K. C., Zhang S. and Lechowicz M. Harsh environmental regimes increase the functional significance of
737 intraspecific variation in plant communities. *Functional Ecology*, 2020, 34, 1666-1677.

738 Niu S. L. Photosynthesis research on the predominant legume species in Hunshandak Sandland. 2004, Graduation
739 Thesis.

740 Qi L. X. Response of leaf traits of *Pinus mongoliensis* and *Pinus massoniana* to elevation gradient in Daiyun
741 Mountain. 2015, Graduation Thesis.

742 Ren Q. J., Li Q. J., Bu H. Y., et al. Comparison of physiological and leaf morphological traits for photosynthesis of
743 the 51 plant species in the Maqu alpine swamp meadow. *Chinese Journal of Plant Ecology*, 2015, 39, 593-603.

744 Ren Y. T. The study of leaf functional traits of typical plants across the Alashan Desert. 2017, Graduation Thesis.

745 Ren Y., Wei C. G. and Guo X. Y. Comparison on leaf function traits of six kinds of plant in Ordos. *Journal of Inner
746 Mongolia Forestry Science & Technology*, 2019, 45, 43-46, 55.

747 Rios R. S., Salgado-Luarte C. and Gianoli E. Species divergence and phylogenetic variation of ecophysiological
748 traits in lianas and trees. *PloS One*, 2007, 9, e99871.

749 Shang K. K. Differentiation and maintenance of relict deciduous broad-leaved forest patterns along micro-
750 topographic gradient in subtropical area, East China. 2011, Graduation Thesis.

751 Song Y T. Study on functional plant ecology in Songnen Grassland Northeast China. 2012, Graduation Thesis.

752 Song Y T., Zhou D. W., Li Q., et al. Leaf nitrogen and phosphorus stoichiometry in 80 herbaceous plant species of
753 Songnen grassland in Northeast China. *Chinese Journal of Plant Ecology*, 2012, 36, 222-230.

754 Tan X. Y. Research on leaf functional diversity of forest communities in rainy area of south-west China. 2014,
755 Graduation Thesis.

756 Tang Q. Q. Variation in functional traits of plants in the Subtropical Evergreen and Deciduous Broad-leaved Mixed
757 Forest. 2016, Graduation Thesis.

758 Tang Y. Inter-specific variations and relationship in leaf traits of major temperate species in northern China. 2011,
759 Graduation Thesis.

760 Tao J. P., Zuo J., He Z., et al. Traits including leaf dry matter content and leaf pH dominate over forest soil pH as
761 drivers of litter decomposition among 60 species. *Functional Ecology*, 2019, 33, 1798-1810.

762 Tian M., Yu G. R., He N. P., et al. Leaf morphological and anatomical traits from tropical to temperate coniferous
763 forests: Mechanisms and influencing factors. *Scientific Reports*, 2016, 6, 19703.

764 Wang B. Analysis of leaf functional traits of 13 species trees in northwestern Fujian Province. 2019, Graduation

765 Thesis.

766 Wang B. B. A study on ecological stoichiometry of six kinds of dominant shrubs in Huangcangyu Nature Reserve.
767 2015, Graduation Thesis.

768 Wang G. H. Leaf trait co-variation, response and effect in a chronosequence. *Journal of Vegetation Science*, 2007,
769 18, 563-570.

770 Wang G. H., Liu J. L. and Meng T. T. Leaf trait variation captures climate differences but differs with species
771 irrespective of functional group. *Journal of Plant Ecology*, 2015, 8, 61-69.

772 Wang J. Y., Wang S. Q., Li R. L., et al. C:N:P stoichiometric characteristics of four forest types' dominant tree species
773 in China. *Chinese Journal of Plant Ecology*, 2011, 35, 587-595.

774 Wang K. B. Vegetation ecological features and net primary productivity simulation in Yanggou watershed in the
775 Loess hill-gully areas of China. 2011, Graduation Thesis.

776 Wang S. S. The traits and adaptive strategies of main herbaceous plants and lianas on micro-topographical units in
777 Longjishan reserves of Anhui Province. 2016, Graduation Thesis.

778 Wei L. P. Variations in functional traits of main tree species along tree-crown in broadleaved Korean Pine Forest in
779 Jiaohe, Jilin Province. 2014, Graduation Thesis.

780 Wei L. P., Hou J. H. and Jiang S. S. Changes of leaf functional traits of two main species along tree height in broad-
781 leaved Korean pine forest. *Guangdong Agricultural Sciences*, 2014, 12, 55-58, 71.

782 Wei L. Y. and Shangguan Z. P. Relation between specific leaf areas and leaf nutrient contents of plants growing on
783 slopelands with different farming-abandoned periods in the Loess Plateau. *Acta Ecologica Sinica*, 2008, 28,
784 2526-2535.

785 Wei L. Y., Zhou J. W., Xiao H. G., et al. Variations in leaf functional traits among plant species grouped by growth
786 and leaf types in Zhenjiang, China. *Journal of Forestry Research*, 2011, 28, 241-248.

787 Wu D. H., Pietsch K. A., Staab M., et al. Wood species identity alters dominant factors driving fine wood
788 decomposition along a subtropical plantation forests tree diversity gradient in subtropical plantation forests.
789 *Biotropica*, 2021, 53, 643-657.

790 Wu T. G., Chen B. F., Xiao Y. H., et al. Leaf stoichiometry of trees in three forest types in Pearl River Delta, South
791 China. *Chinese Journal of Plant Ecology*, 2009, 34, 58-63.

792 Xie Y. J. The characteristics of 20 dominant plant functional traits in evergreen broad-leaf forest in Daming Mountain
793 Nature Reserve, Guangxi. 2013, Graduation Thesis.

794 Xu M. F., Ke X. H., Zhang Y., et al. Wood densities of six hardwood tree species in Eastern Guangdong and
795 influencing factors. *Journal of South China Agricultural University*, 2016, 37, 100-106.

796 Xu M. S., Zhao Y. T., Yang X. D., et al. Geostatistical analysis of spatial variations in leaf traits of woody plants in
797 Tiantong, Zhejiang Province. *Chinese Journal of Plant Ecology*, 2016, 40, 48-59.

798 Xu Y. Z. Biomass estimate and storage mechanisms in northern subtropical forest ecosystems, central China. 2016,
799 Graduation Thesis.

800 Xun Y. H., Di X. Y. and Jin G. Z. Vertical variation and economic strategy of leaf trait of major tree species in a
801 typical mixed broadleaved-Korean pine forest. *Chinese Journal of Plant Ecology*, 2020, 44, 730-741.

802 Yan E. R., Wang X. H., Guo M., et al. C:N:P stoichiometry across evergreen broad-leaved forests, evergreen
803 coniferous forests and deciduous broad-leaved forests in the Tiantong region, Zhejiang Province, eastern China.
804 *Chinese Journal of Plant Ecology*, 2010, 34, 48-57.

805 Yang S. The adaptive strategies of main herbaceous plants traits to different micro-topographical units in Dashushan
806 Mountain, Hefei. 2017, Graduation Thesis.

807 Yang Y., Xu X., Xu M., et al. Adaptation strategies of three dominant plants in the trough-valley karst region of
808 northern Guizhou Province, Southwestern China, evidence from associated plant functional traits and

809 ecostoichiometry. *Earth and Environment*, 2020, 48, 413-423.

810 Yang Z., Fan S. X., Zhou B. C., et al. Leaf function and soil nutrient differences of dominant tree species on different
811 slope aspects at the south foothills of Taihang Mountains. *Journal of Henan Agricultural University*, 2020, 54,
812 408-414.

813 Yin Q. L., Wang L., Lei, M. L., et al. The relationships between leaf economics and hydraulic traits of woody plants
814 depend on water availability. *Science of the Total Environment*, 2018, 621, 245-252.

815 Yu Y. H., Zhong X. P. and Chen W. Analysis of relationship among leaf functional traits and economics spectrum of
816 dominant species in northwestern Guizhou Province. *Journal of Forest and Environment*, 2018, 38, 196-201.

817 Yuan S. Preliminary research on plant functional traits and the capability of carbon sequestration of major tree species
818 in Changbai Mountain Area. 2011, Graduation Thesis.

819 Zhang H., Chen H. Y. H., Lian J. Y., et al. Using functional trait diversity patterns to disentangle the scale-dependent
820 ecological processes in a subtropical forest. *Functional Ecology*, 2018, 32, 1379-1389.

821 Zhang J. G., Fu S. L., Wen Z. D., et al. Relationship of key leaf traits of 16 woody plant species in Low Subtropical
822 China. *Journal of Tropical and Subtropical Botany*, 2009, 17, 395-400.

823 Zhang J. L., Poorter L., Cao K. F. Productive leaf functional traits of Chinese savanna species. *Plant Ecology*, 2012,
824 213, 1449-1460.

825 Zhang J. Y. Comparative study on the different plant functional groups leaf traits at the Maoershan Region. 2008,
826 Graduation Thesis.

827 Zhang Q. W., Zhu S. D., Jansen S., et al. Topography strongly affects drought stress and xylem embolism resistance
828 in woody plants from a karst forest in Southwest China. *Functional Ecology*, 2020, 35, 566-577.

829 Zhang S. B. and Cao K. F. Stem hydraulics mediates leaf water status, carbon gain, nutrient use efficiencies and
830 plant growth rates across dipterocarp species. *Functional Ecology*, 2009, 23, 658-667.

831 Zhang S. B., Cao K. F., Fan Z. X., et al. Potential hydraulic efficiency in angiosperm trees increases with growth-
832 site temperature but has no trade-off with mechanical strength. *Global Ecology and Biogeography*, 2013, 22,
833 971-981.

834 Zhang Y., Ren Y. X., Yao J., et al. Leaf nitrogen and phosphorous stoichiometry of trees in *Pinus tabulaeformis* Carr
835 stands, North China. *Journal of Anhui Agricultural University*, 2012, 39, 247-251.

836 Zhao Y. T., Ali, A. and Yan, E. R. The plant economics spectrum is structured by leaf habits and growth forms across
837 subtropical species. *Tree Physiology*, 2016, 37, 173-185.

838 Zheng X. J., Li S. and Li Y. Leaf water uptake strategy of desert plants in the Junggar Basin, China. *Chinese Journal*
839 *of Plant Ecology*, 2011, 35, 893-905.

840 Zheng Y. M. Carbon, nitrogen and phosphorus stoichiometry of plant and soil in the sandy hills of Poyang Lake.
841 2014, Graduation Thesis.

842 Zheng Z. X. Comparison of plant leaf, height and seed functional traits in dry-hot valleys. 2010, Graduation Thesis.

843 Zhou J. Y., He J. J., Guo Z. Y., et al. A study on specific leaf area and leaf dry matter content of five dominant species
844 in Xiangshan Mountain, Huaibei City, Anhui Province. *Journal of Huaibei Normal University (Natural*
845 *Sciences)*, 2013, 34, 51-54.

846 Zhou X., Zuo X. A., Zhao X. Y., et al. Plant functional traits and interrelationship of 34 plant species in south central
847 Horqin Sandy Land, China. *Journal of Desert Research*, 2015, 35, 1489-1495.

848 Zhu B. R., Xu B. and Zhang D. Y. Extent and sources of variation in plant functional traits in grassland. *Journal of*
849 *Beijing Normal University (Natural Science)*, 2011, 47, 485-489.

850 Zhu S. D., Song J. J., Li R. H., et al. Plant hydraulics and photosynthesis of 34 woody species from different
851 successional stages of subtropical forests. *Plant Cell and Environment*, 2013, 36, 879-891.

852 Zhu X B, Liu Y. M. and Sun S. C. Leaf expansion of the dominant woody species of three deciduous oak forests in

854 **Appendix B**

855 **Table B1** Summary of statistics in plant functional traits, environmental variables and geographical
 856 distribution in China.

Trait	Unit	Range	Mean	CV (%)	No. of species	Entries	Sites
SLA	m ² kg ⁻¹	0.06–81.68	17.88	54.96	2463	9195	1032
LDMC	g g ⁻¹	0.06–0.95	0.34	100.00	1582	3957	193
LNC	mg g ⁻¹	3.41–66.02	21.52	37.44	2335	7407	567
LPC	mg g ⁻¹	0.09–9.70	1.83	62.19	2074	6266	515
LA	cm ²	0.0033–2553.33	36.16	259.64	1838	5976	691
WD	g cm ⁻³	0.25–1.37	0.68	33.16	768	1788	639
Altitude	m	-144–5454					1430
MAT	°C	-12.07–24.32					1430
MAP	mm	15–2982					1430
Soil total N	g kg ⁻¹	0.11–10.25					1430
Bulk density	g cm ⁻³	0.83–1.45					1430

857 SLA, specific leaf area; LDMC, leaf dry matter content; LNC, leaf N concentration; LPC, leaf P concentration; LA,
 858 leaf area; WD, wood density; MAT, mean annual temperature; MAP, mean annual precipitation.

859 **Table B2** List of all the predictors including environment and remote sensing variables used in this study.

Type of variables	Variable name	Abbreviations	Units	Time periods	Spatial resolution	Source
Climate	Mean annual temperature	MAT	°C	1970-2000	1 km	WorldClim version 2.1
	Mean diurnal range	MDR	°C	1970-2000	1 km	WorldClim version 2.1
	Temperature seasonality	TS	°C	1970-2000	1 km	WorldClim version 2.1
	Max temperature of warmest month	Tmin	°C	1970-2000	1 km	WorldClim version 2.1
	Min temperature of coldest month	Tmax	°C	1970-2000	1 km	WorldClim version 2.1
	Temperature annual range	TAR	°C	1970-2000	1 km	WorldClim version 2.1
	Isothermality	IS	%	1970-2000	1 km	WorldClim version 2.1
	Mean temperature of wettest quarter	MTEQ	°C	1970-2000	1 km	WorldClim version 2.1
	Mean temperature of driest quarter	MTDQ	°C	1970-2000	1 km	WorldClim version 2.1
	Mean temperature of warmest quarter	MTWQ	°C	1970-2000	1 km	WorldClim version 2.1
	Mean temperature of coldest quarter	MTCQ	°C	1970-2000	1 km	WorldClim version 2.1
	Mean annual precipitation	MAP	mm	1970-2000	1 km	WorldClim version 2.1
	Precipitation of wettest month	PEM	mm	1970-2000	1 km	WorldClim version 2.1
	Precipitation of driest month	PDM	mm	1970-2000	1 km	WorldClim version 2.1
	Precipitation seasonality	PS	%	1970-2000	1 km	WorldClim version 2.1
	Precipitation of wettest quarter	PEQ	mm	1970-2000	1 km	WorldClim version 2.1
	Precipitation of driest quarter	PDQ	mm	1970-2000	1 km	WorldClim version 2.1
	Precipitation of warmest quarter	PWQ	mm	1970-2000	1 km	WorldClim version 2.1
	Precipitation of coldest quarter	PCQ	mm	1970-2000	1 km	WorldClim version 2.1
	Aridity index	AI	/	1970-2000	1 km	Global CGIAR-CSI
Solar radiation	RAD	kJ m ⁻² day ⁻¹	1970-2000	1 km	WorldClim version 2.1	
Topography	Elevation	/	m		1 km	SRTM 90m V4.1
Soil	Soil sand content	SAND	%	/	1 km	Shangguan et al. (2013)
	Soil silt content	SILT	%	/	1 km	Shangguan et al. (2013)
	Soil clay content	CLAY	%	/	1 km	Shangguan et al. (2013)
	Bulk density	BD	g cm ⁻³	/	1 km	Shangguan et al. (2013)
	Soil pH	pH	/	/	1 km	Shangguan et al. (2013)

Continued

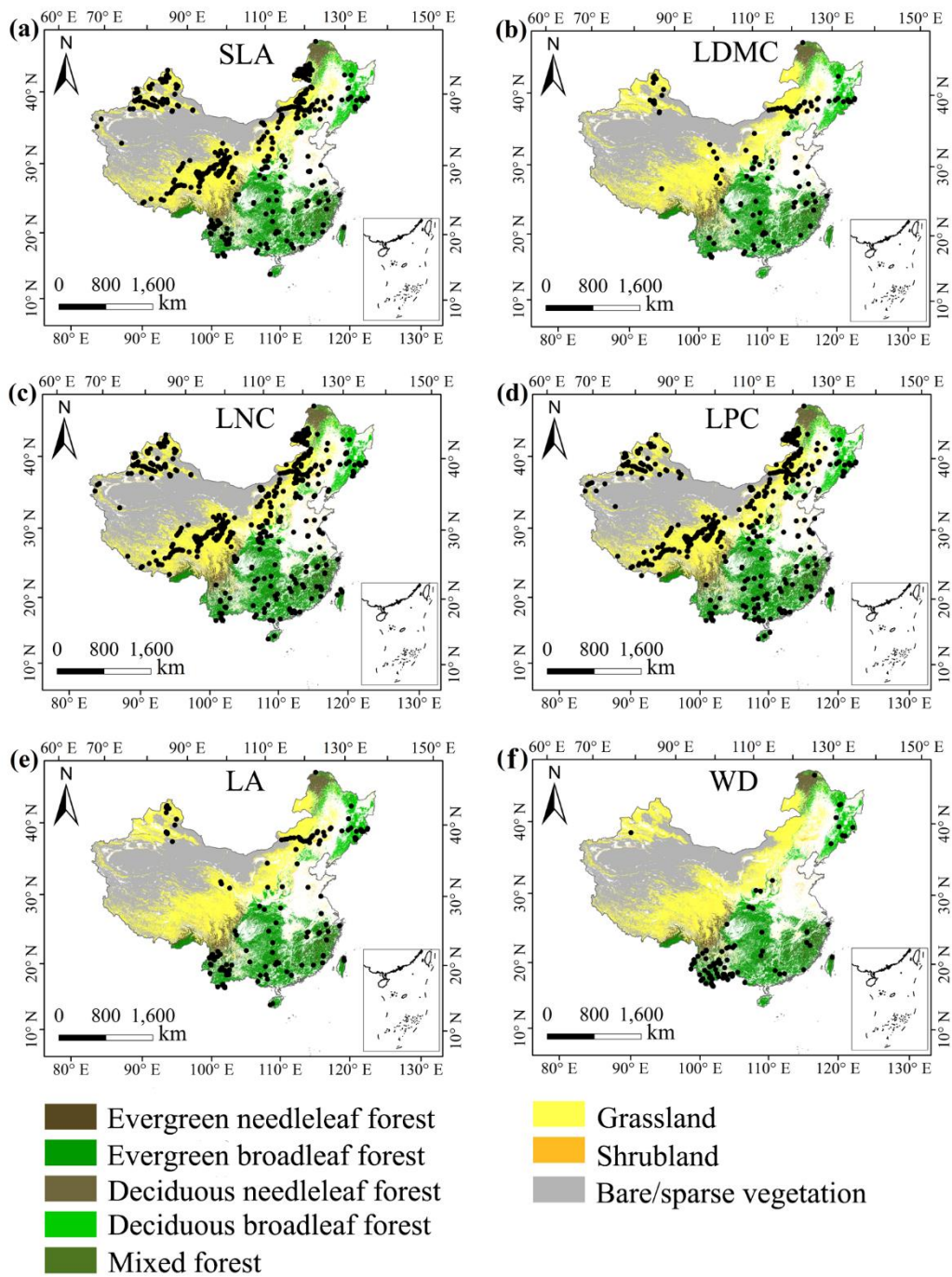
Type of variables	Variable name	Abbreviations	Units	Time periods	Spatial resolution	Source
	Soil organic matter	SOC	g kg ⁻¹	/	1 km	Shangguan et al. (2013)
	Soil total N	STN	g kg ⁻¹	/	1 km	Shangguan et al. (2013)
	Soil total P	STP	g kg ⁻¹	/	1 km	Shangguan et al. (2013)
	Soil alkali-hydrolysable N	SAN	mg kg ⁻¹	/	1 km	Shangguan et al. (2013)
	Soil available P	SAP	mg kg ⁻¹	/	1 km	Shangguan et al. (2013)
	Soil available K	SAK	mg kg ⁻¹	/	1 km	Shangguan et al. (2013)
	Cation exchange capacity	CEC	me kg ⁻¹	/	1 km	Shangguan et al. (2013)
EVI	MODIS EVI long-term monthly averages		/	2001-2018	1 km	MOD13A3 V006
NIR	MODIS NIR long-term monthly averages		/	2001-2018	1 km	MOD13A3 V006
MIR	MODIS MIR long-term monthly averages		/	2001-2018	1 km	MOD13A3 V006
Red	MODIS red long-term monthly averages		/	2001-2018	1 km	MOD13A3 V006
Blue	MODIS blue long-term monthly averages		/	2001-2018	1 km	MOD13A3 V006
MTCI	MTCI long-term monthly averages		/	2003-2011	4.63 km	MTCI level 3 product
Land cover	Land cover map		/	2015	100 m	Copernicus Global Land Service Collection 3

860 The remote sensing variables are calculated as long-term monthly averages from 2001 to 2018. Thus 12 variables of
861 each remote sensing category are obtained.

862 **Table B3** The number of samples of eight plant functional trait used for model training (80%) and
 863 validation (20%).

Traits	No. of samples	No. of samples used for model training	No. of samples used for model validation
SLA	9195	7356	1839
LDMC	3957	3166	791
LNC	7407	5926	1481
LPC	6266	5013	1253
LA	5976	4781	1195
WD	1787	1430	357

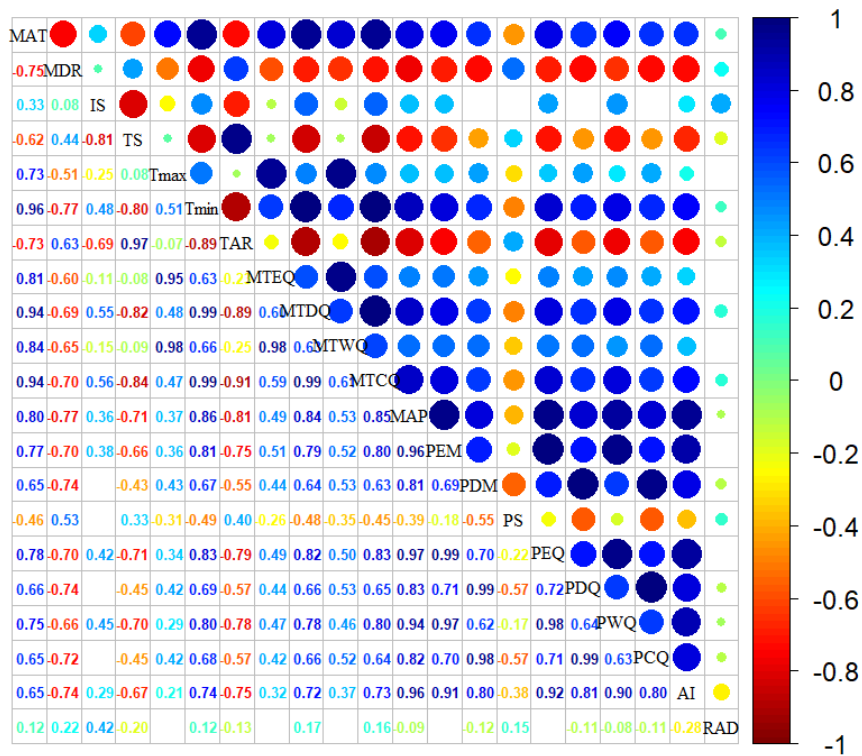
864 SLA, specific leaf area ($\text{m}^2 \text{kg}^{-1}$); LDMC, leaf dry matter content (g g^{-1}); LNC, leaf N concentration (mg
 865 g^{-1}); LPC, leaf P concentration (mg g^{-1}); LA, leaf area (cm^2); WD, wood density (g cm^{-3}).



866

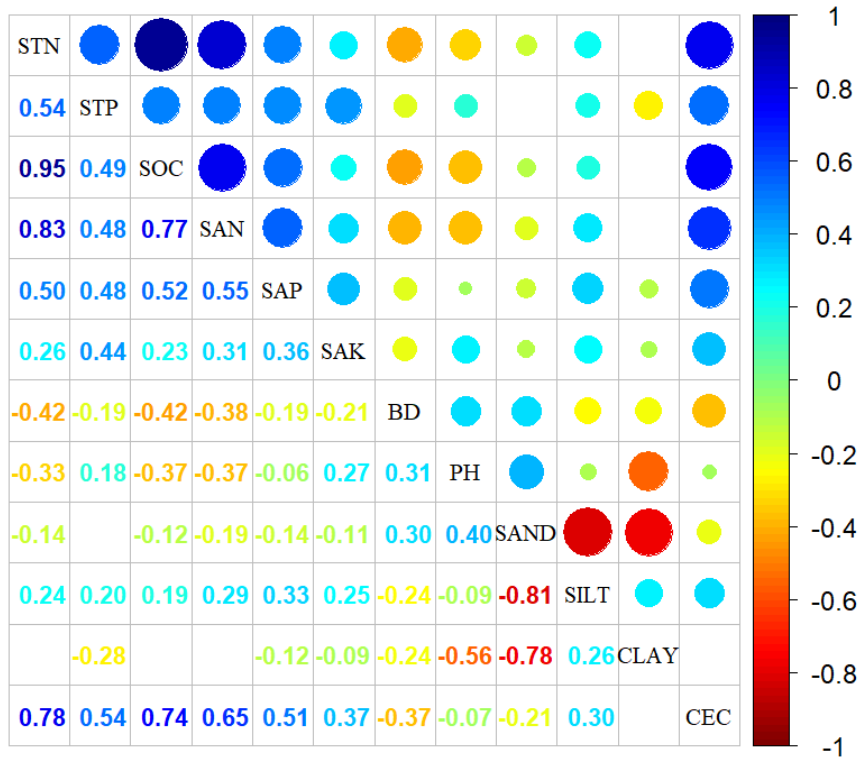
867 **Figure B1.** The distribution of sampling site of each plant functional traits across China. The black

868 dots represented the locations of trait observations.



869

870 **Figure B2.** Correlations among climate variables. The blank indicates that the correlations are not
 871 significant ($P > 0.05$). The size of the circles is proportional to the correlation coefficient. The
 872 abbreviation of climate variables is seen in Table B2.



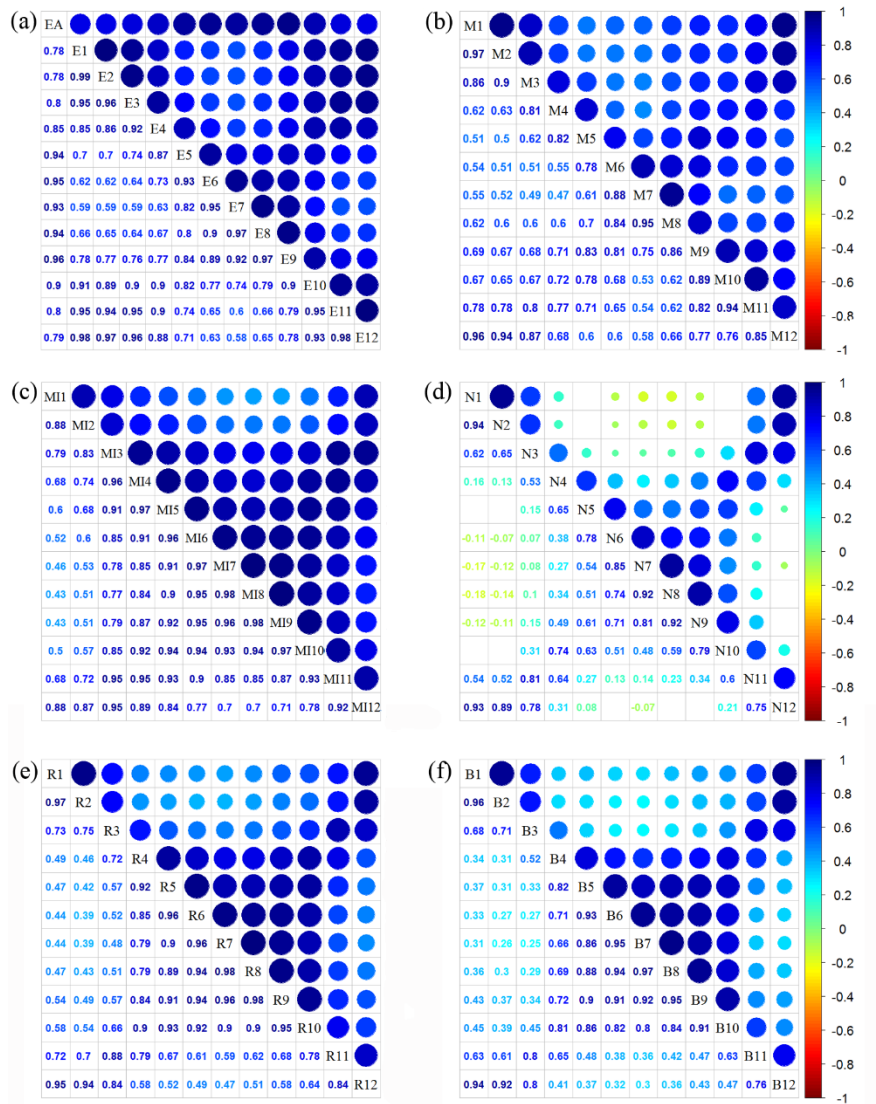
873

874

875

876

Figure B3. Correlations among soil variables. The blank indicates that the correlations are not significant ($P > 0.05$). The size of the circles is proportional to the correlation coefficient. The abbreviation of soil variables is seen in Table B2.



877

878 **Figure B4.** Correlations among monthly remote sensing variables. The blank indicates that the
 879 correlations are not significant ($P > 0.05$). The size of the circles is proportional to the correlation
 880 coefficient. (a) enhanced vegetation index (EVI); (b) MERIS terrestrial chlorophyll index (MTCI);
 881 (c) MIR reflectance; (d) NIR reflectance; (e) red reflectance; (f) blue reflectance.

882 **Appendix C**

883 **Table C1** Optimal parameter combination and model performance of random forest for plant functional
 884 traits

Traits	n.tree	mtry	R ²	NRMSE	MAE
SLA	1000	24	0.476	0.22	5.134
LDMC	1000	11	0.234	0.20	0.072
LNC	1000	57	0.392	0.00	0.098
LPC	1000	20	0.587	0.05	0.129
LA	1000	18	0.278	0.48	26.622
WD	1000	9	0.531	0.02	0.072

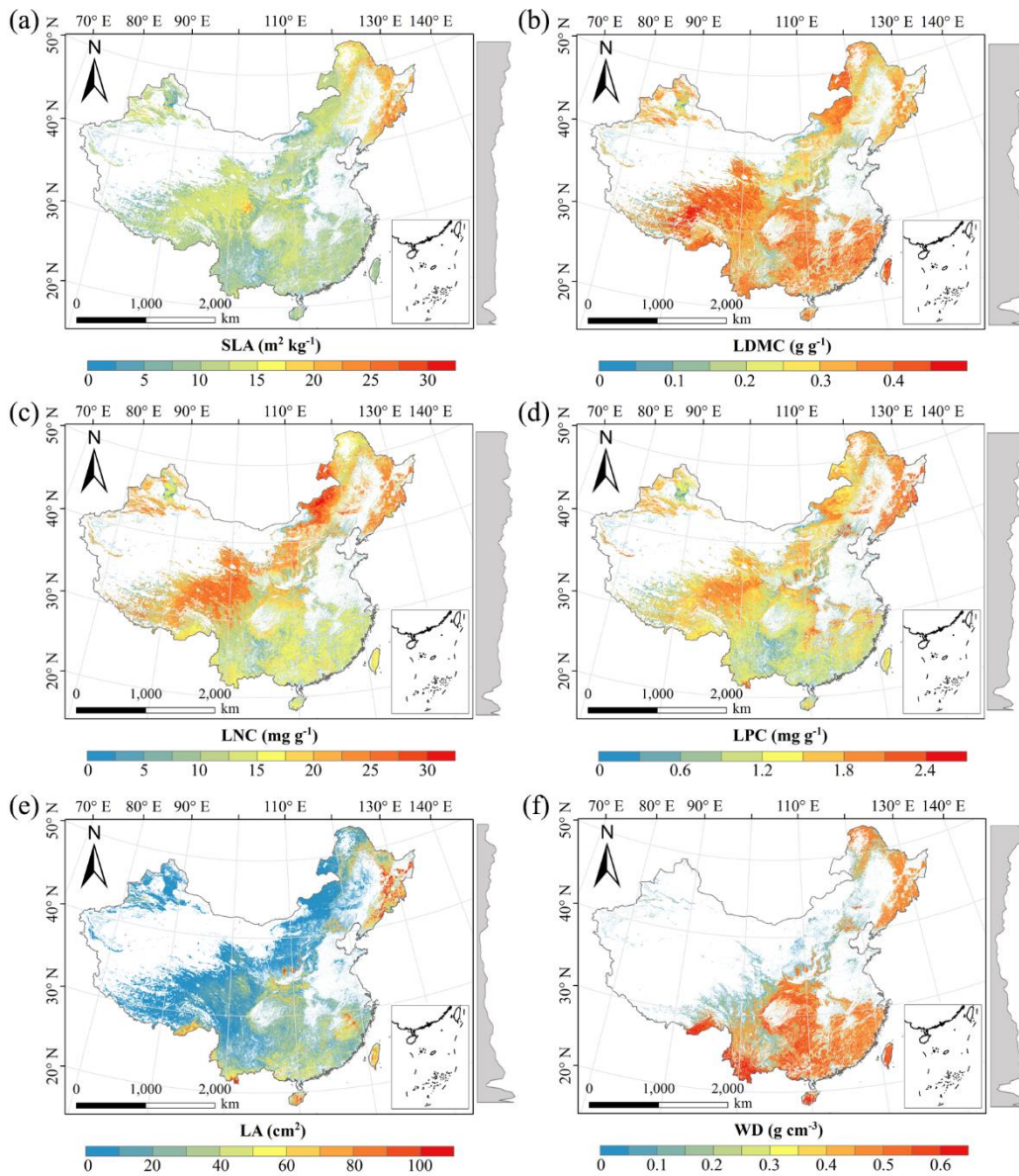
885 SLA, specific leaf area; LDMC, leaf dry matter content; LNC, leaf N concentration; LPC, leaf P
 886 concentration; LA, leaf area; WD, wood density.

887

888 **Table C2** Optimal parameter combination and model performance of boosted regression trees for plant
 889 functional traits

Traits	n.tree	interaction. depth	shrinkage	learning rate	bag fractions	R ²	NRMSE	MAE
SLA	3000	6	0.01	10	0.75	0.486	0.20	5.082
LDMC	3000	2	0.01	10	0.75	0.247	0.19	0.071
LNC	3000	6	0.01	10	0.70	0.414	0.00	0.096
LPC	3000	7	0.01	10	0.75	0.591	0.05	0.129
LA	3000	3	0.001	10	0.75	0.282	0.55	27.556
WD	3000	4	0.01	10	0.70	0.627	0.01	0.066

890 SLA, specific leaf area; LDMC, leaf dry matter content; LNC, leaf N concentration; LPC, leaf P
 891 concentration; LA, leaf area; WD, wood density.



893

894

Figure D1. Spatial distribution of plant functional traits based on random forest. The grey curves

895

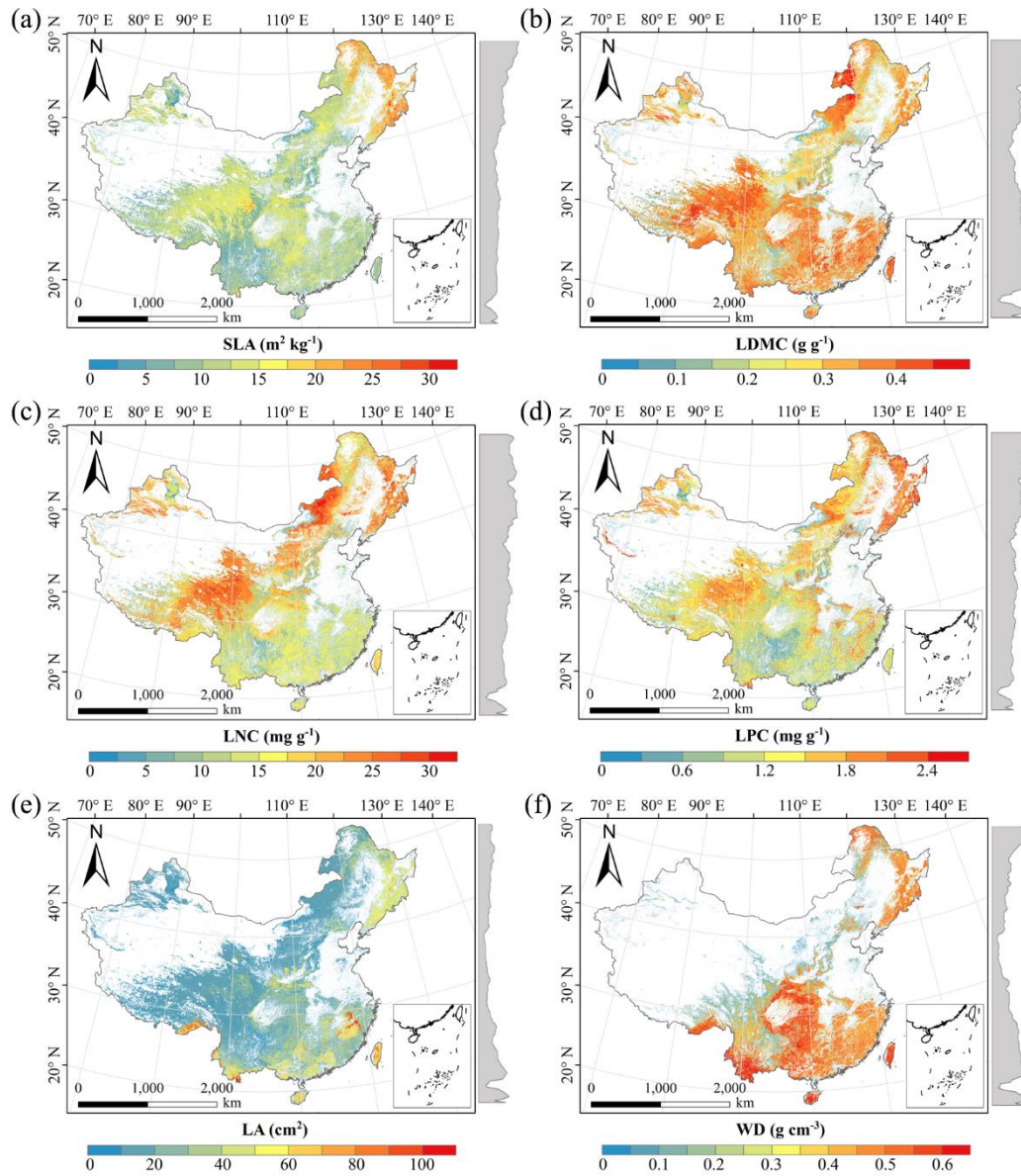
on the right of maps were trait distribution along with latitude. SLA, specific leaf area; LDMC, leaf

896

dry matter content; LNC, leaf N concentration; LPC, leaf P concentration; LA, leaf area; WD, wood

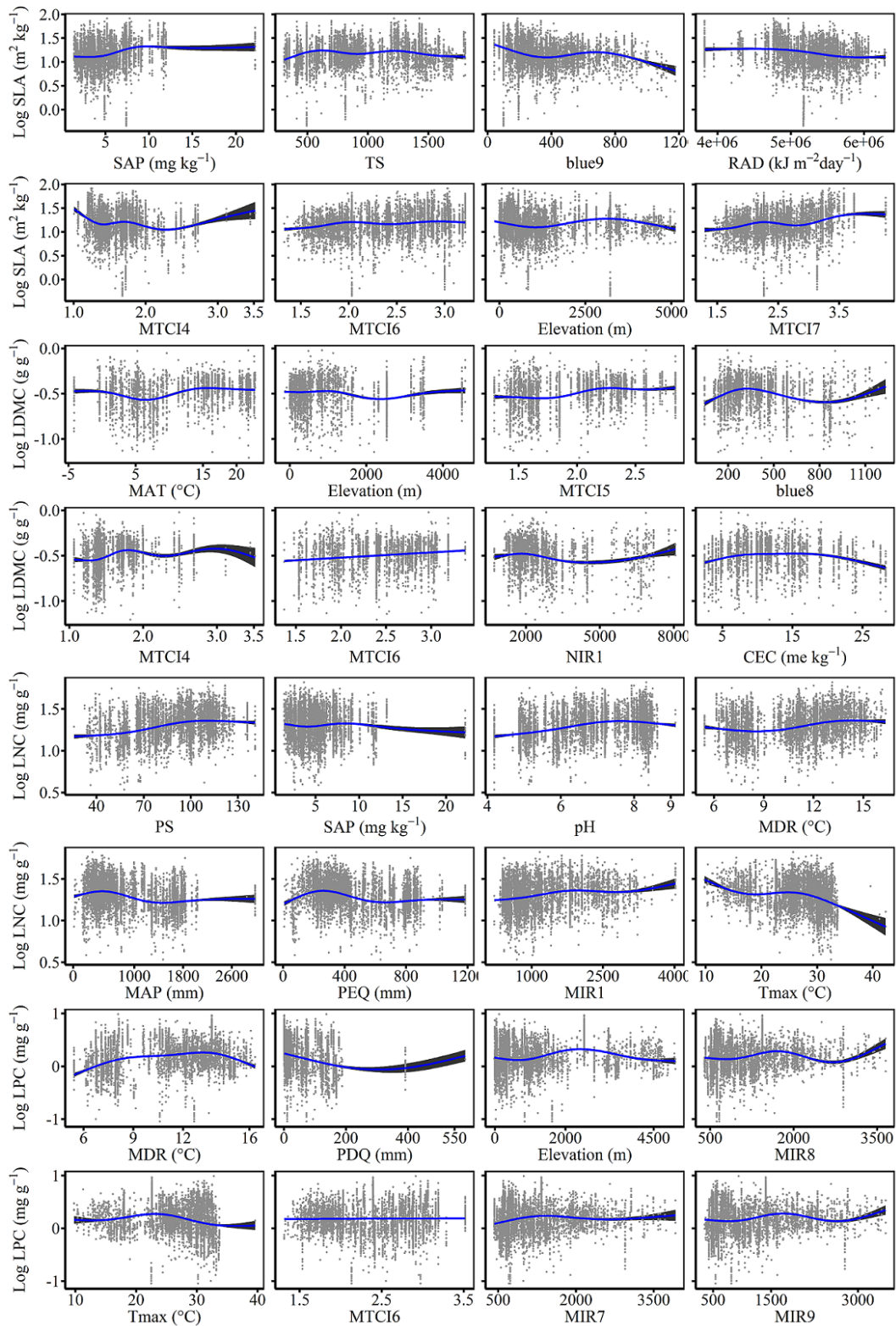
897

density.

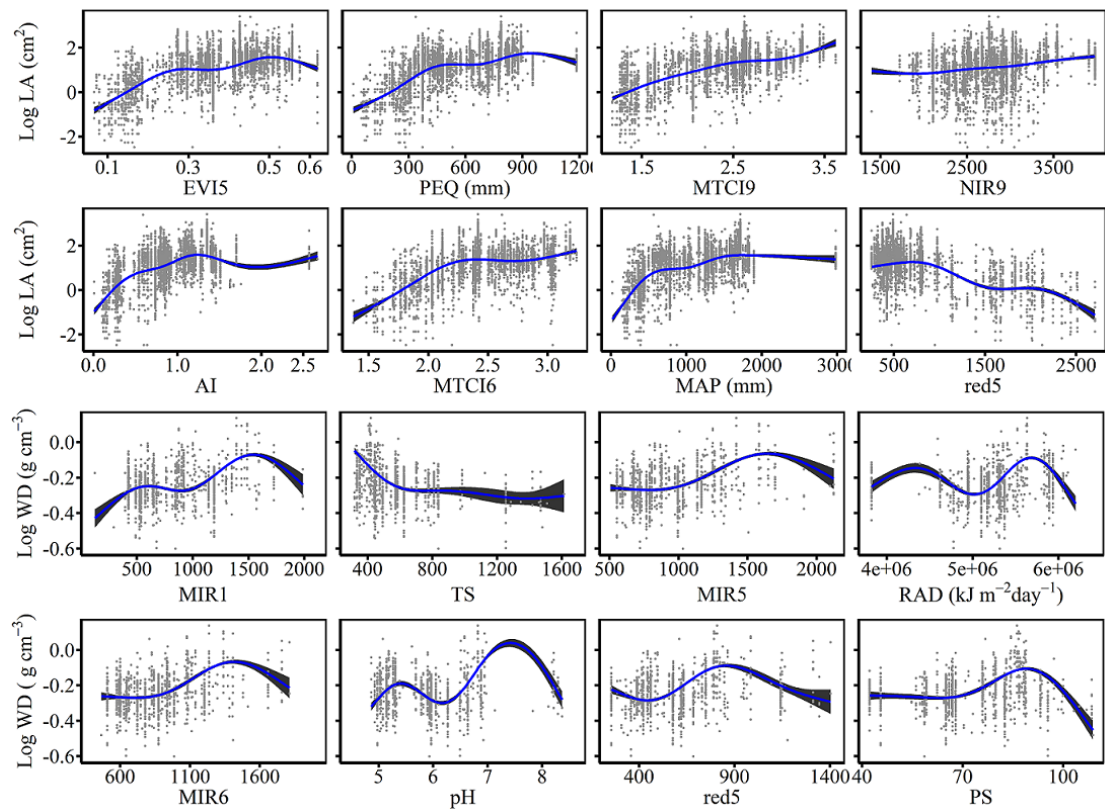


898

899 **Figure D2.** Spatial distribution of plant functional traits based on boosted regression trees. The grey
 900 curves on the right of maps were trait distribution along with latitude. SLA, specific leaf area;
 901 LDMC, leaf dry matter content; LNC, leaf N concentration; LPC, leaf P concentration; LA, leaf
 902 area; WD, wood density.



904
 905 **Figure E1.** The relationships between SLA (specific leaf area), LDMC (leaf dry matter content),
 906 LNC (leaf N concentration), LPC (leaf P concentration) and their eight most important predictors.



907

908

Figure E2. The relationships between LA (leaf area), WD (wood density) and their eight most

909

important predictors.

910 **Appendix F Comparisons between our study with trait maps from previous studies**

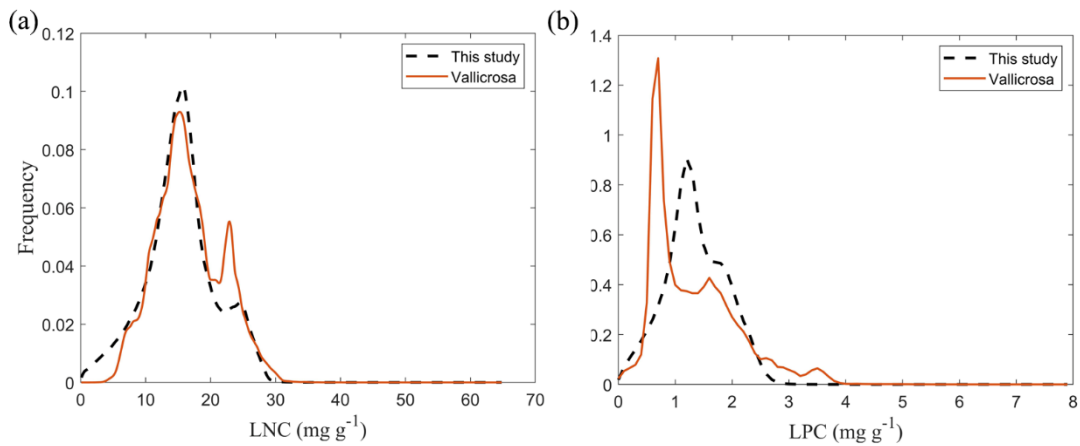
911 Given that the trait maps predicted for China were not available from the literature and authors,
 912 we compared our study with those studies performed at the global scale (see Table F1). Thus, we
 913 extracted the data in China from global trait maps. Before the quantitative comparisons with
 914 previous studies, we performed two steps to make the data products as comparable as possible and
 915 improve the consistency between different studies. First, due to different spatial resolution of global
 916 trait maps (mainly 0.5°) and our study, we resampled the data products of previous studies and our
 917 maps to 0.5° spatial resolution. In addition, Vallicrosa et al. (2022) generated the global maps of
 918 LNC and LPC with a 1 km spatial resolution, we also compared the frequency distribution of
 919 Vallicrosa et al. (2022) with that of our study at a 1 km spatial resolution. Second, our study focused
 920 on natural vegetation, so the global trait maps were used to filter out non-natural vegetation (e.g.,
 921 croplands). For example, Madani et al. (2018) predicted the spatial distributions of SLA that
 922 included croplands. We quantitatively compared our maps with previous studies from two
 923 perspectives. The comparisons among trait maps were made using frequency plots and spatial
 924 correlations (Figure 7 and Table 5). And the maps of spatial differences between our study and
 925 previous studies were displayed as Figs F1-F5 in Appendix F.

926 **Table F1.** Summary table of related trait maps of previous studies used in this study.

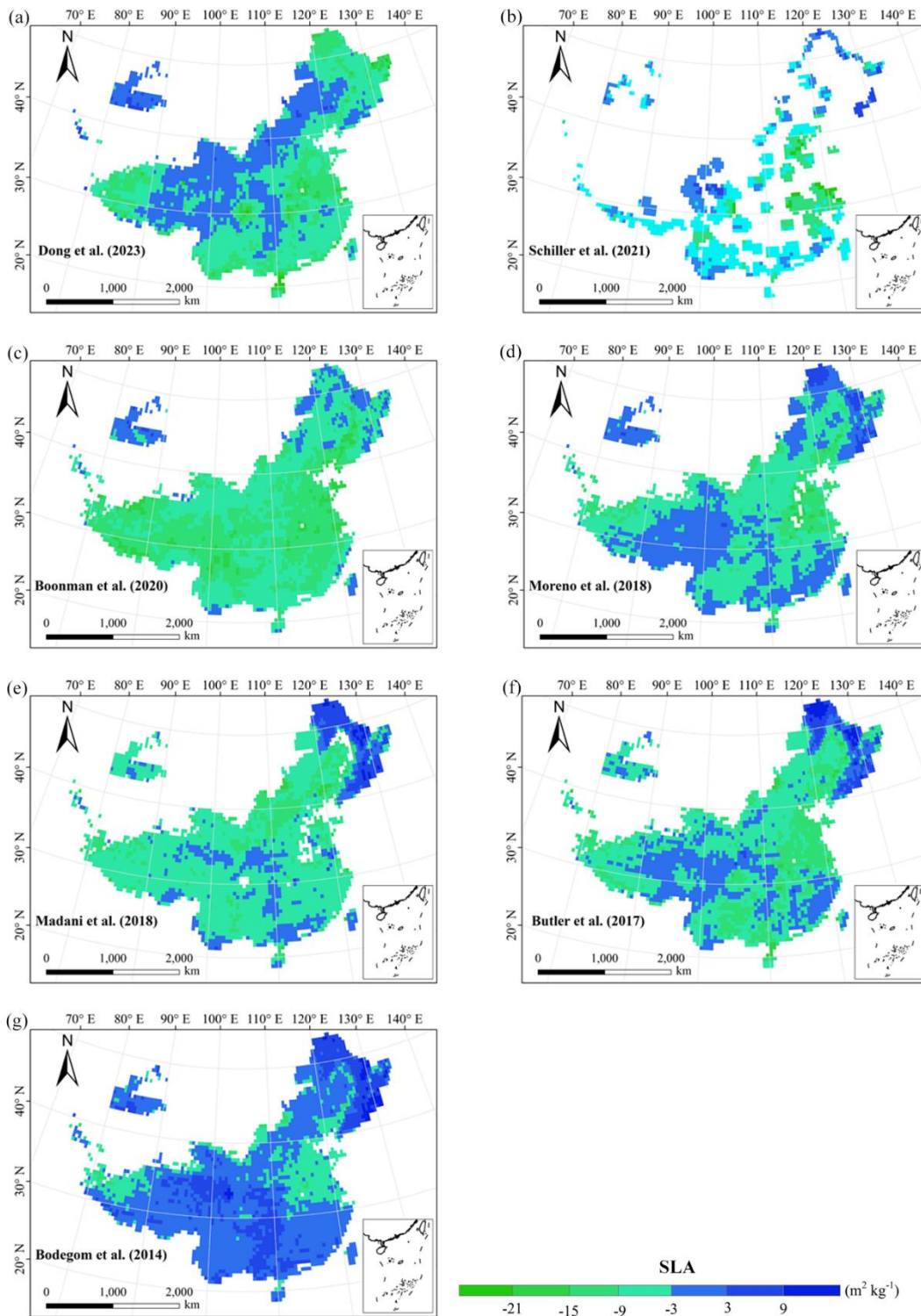
References	Related traits	Methods	Predictors	Consideration of PFT	Resolution
Dong et al. (2023)	SLA LNC	Optimality models	Climate	Yes	0.5°
Vallicrosa et al. (2022)	LNC LPC	Neural networks	Climate Soil N and P deposition	Yes	0.0083°
Schiller et al. (2021)	SLA LNC LA WD	Convolutional Neural Networks	Climate In-situ RGB images	No	0.5°
Boonman et al. (2020)	SLA LNC WD	Generalized linear model, Generalized additive model, Random forest, Boosted regression trees, Ensemble model	Climate Soil	No	0.5°
Moreno et al. (2018)	SLA LNC LPC LDMC	Regularized regression, Random forest, Neural networks, Kernel networks	Climate Elevation Reflectance	Yes	0.0045°
Madani et al.	SLA	Generalized additive	Climate	No	0.5°

(2018)			model			
Butler et al.	SLA	Bayesian model	Climate	Yes	0.5°	
(2017)	LNC		Soil			
	LPC					
Bodegom et al.	SLA	Multiple regression	Climate	No	0.5°	
(2014)	WD	analysis	Soil			

927 The resolutions 0.5°, 0.0083° and 0.0045° correspond to square grid cell sizes of about 50 km, 1 km and
928 500 m at the equator. PFT, plant functional type; SLA, specific leaf area; LDMC, leaf dry matter content;
929 LNC, leaf N concentration; LPC, leaf P concentration; LA, leaf area; WD, wood density.
930

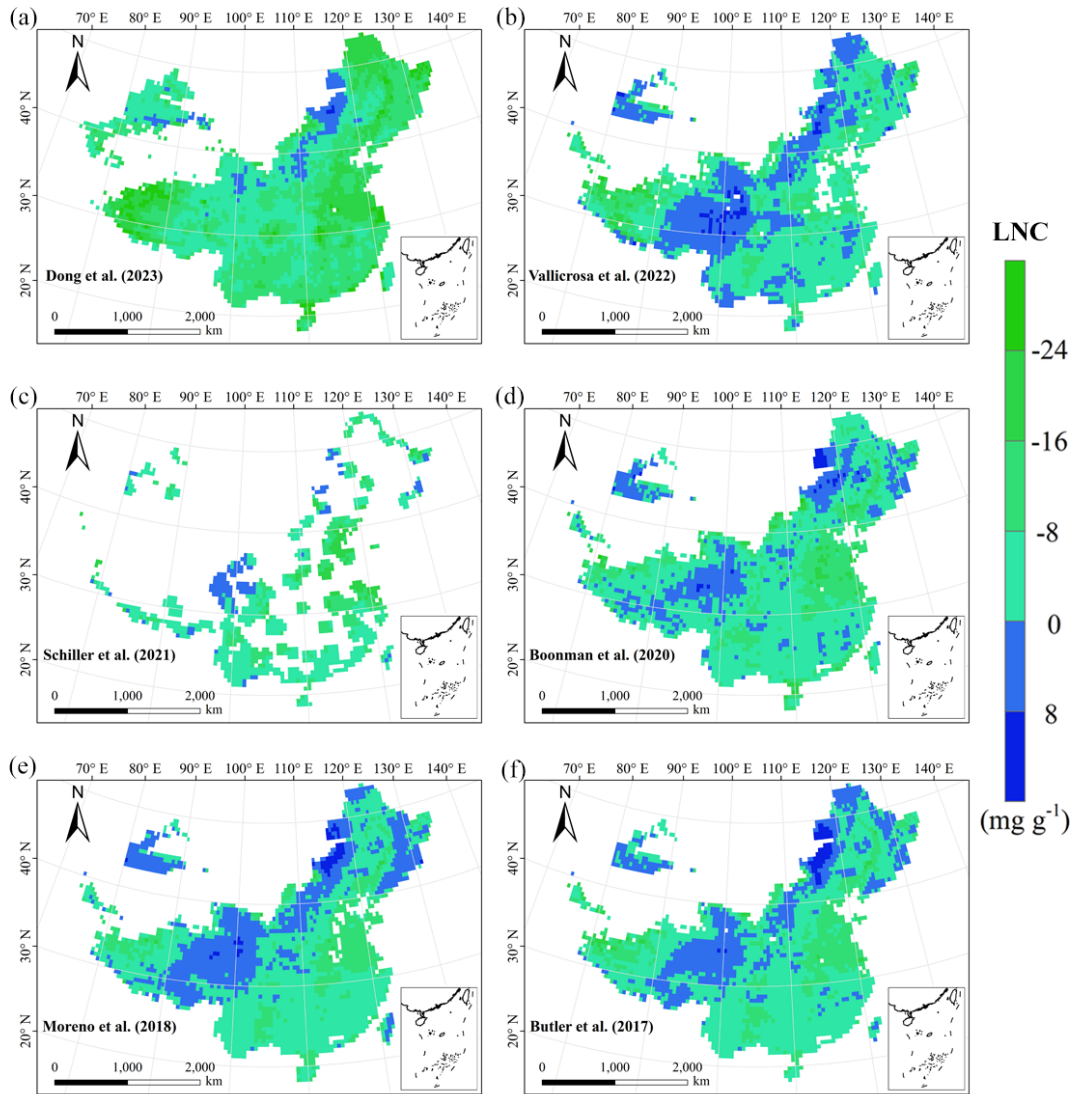


931
932 **Figure F1.** Frequency distributions of plant functional traits in our study (“This study”, dashed black
933 lines) and Vallicrosa et al. (2022) at 1 km spatial resolution. LNC, leaf N concentration (mg g⁻¹);
934 LPC, leaf P concentration (mg g⁻¹).



935
936
937

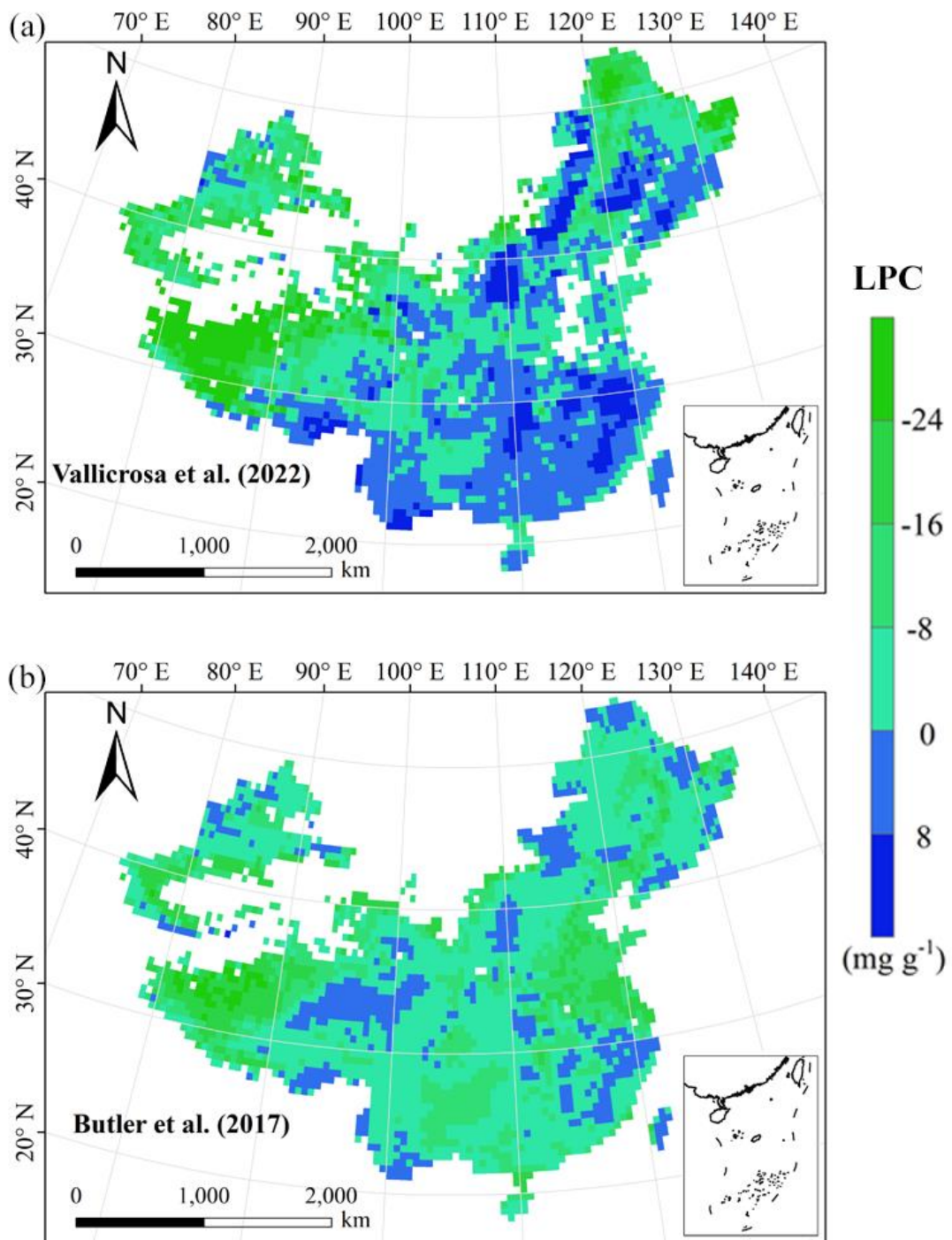
Figure F2. Spatial differences in SLA (specific leaf area, $\text{m}^2 \text{kg}^{-1}$) between our study and trait maps from previous studies (see Table F1 for citations).



938

939 **Figure F3.** Spatial differences in LNC (leaf N concentration, mg g^{-1}) between our study and trait maps

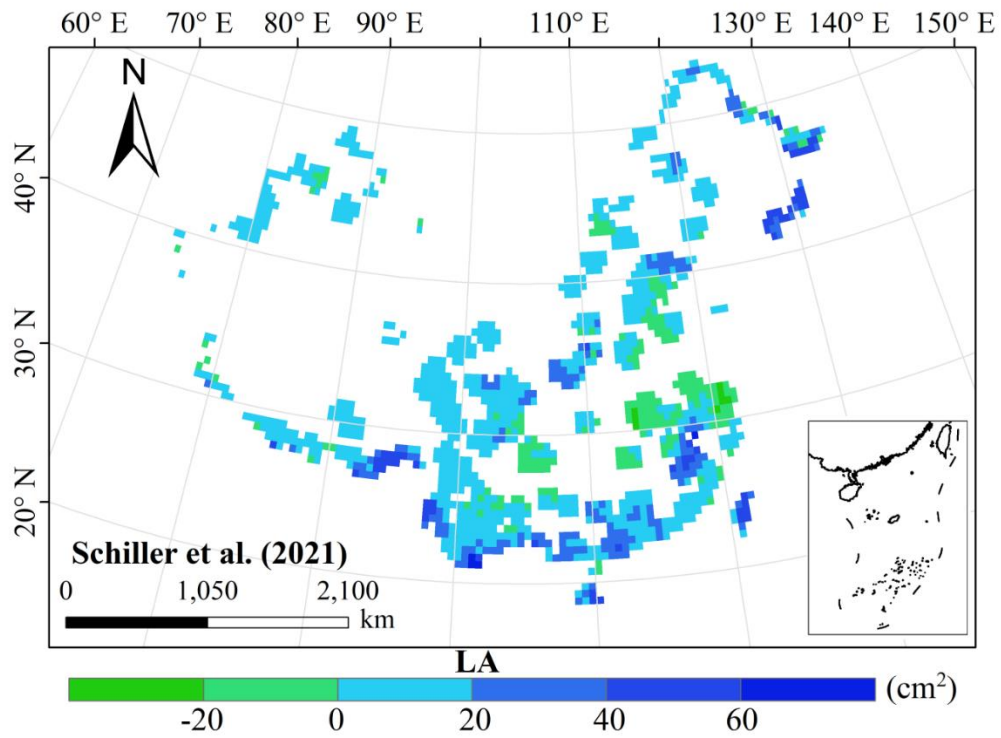
940 from previous studies (see Table F1 for citations).



941

942 **Figure F4.** Spatial differences in LPC (leaf P concentration, mg g⁻¹) between our study and trait maps

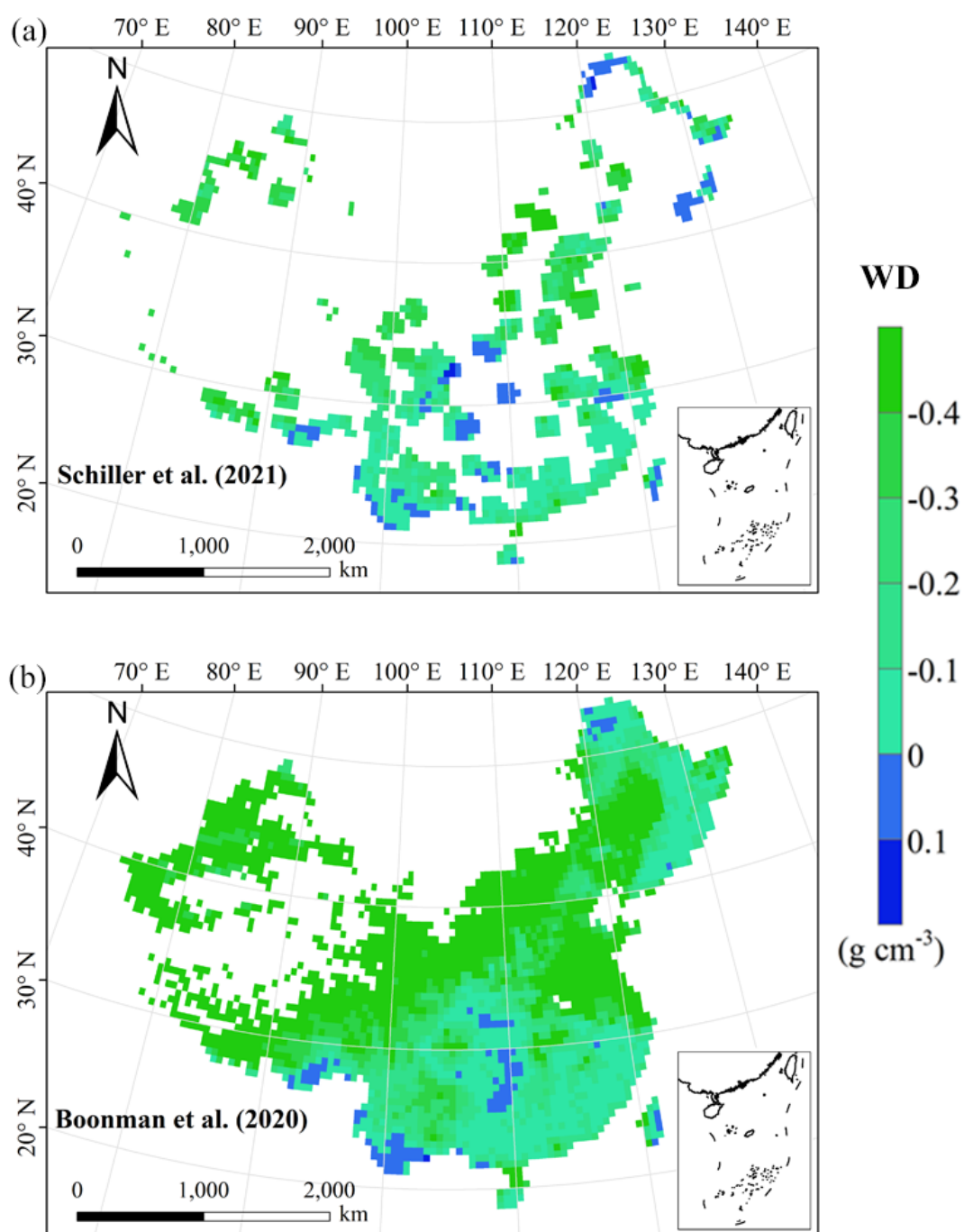
943 from previous studies (see Table F1 for citations).



944

945 **Figure F5.** Spatial differences in LA (leaf area, cm²) between our study and trait maps from previous

946 studies (see Table F1 for citations).



947

948 **Figure F6.** Spatial differences in WD (wood density, g cm^{-3}) between our study and trait maps from
 949 previous studies (see Table F1 for citations).

950 **Author contributions.** NA and NL designed the research. NA did the analysis, processed the data
951 and wrote the draft of the paper. All co-authors commented on the manuscript and agreed upon the
952 final version of the paper.

953
954 **Competing interests.** The contact author has declared that none of the authors has any competing
955 interests.

956
957 **Disclaimer.** Publisher's note: Copernicus Publications remains neutral with regard to jurisdictional
958 claims in published maps and institutional affiliations.

959
960 **Acknowledgement.** We acknowledge financial supports from the National Natural Science
961 Foundation of China (41991234) and the Joint CAS-MPG Research Project (HZXM20225001MI).

962
963 **Financial support.** This work has been supported by the National Natural Science Foundation of
964 China (grant no. 41991234) and the Joint CAS-MPG Research Project (grant no.
965 HZXM20225001MI).

966

967 **References**

968 Ali, A. M., Darvishzadeh, R., Skidmore, A. K., van Duren, I., Heiden, U., and Heurich, M.:
969 Estimating leaf functional traits by inversion of PROSPECT: assessing leaf dry matter content
970 and specific leaf area in mixed mountainous forest. *Int. J. Appl. Earth Obs. Geoinf.*, 45, 66–76,
971 <https://doi.org/10.1016/j.jag.2015.11.004>, 2016.

972 An, N. N., Lu, N., Fu, B. J., Wang, M. Y., and He, N. P.: Distinct responses of leaf traits to
973 environment and phylogeny between herbaceous and woody angiosperm species in China.
974 *Front. Plant Sci.* 12, 799401, <https://doi.org/10.3389/fpls.2021.799401>, 2021.

975 Bakker, M. A., Carreño-Rocabado, G., and Poorter, L.: Leaf economics traits predict litter
976 decomposition of tropical plants and differ among land use types. *Funct. Ecol.*, 25, 473–483,
977 <https://doi.org/10.1111/j.1365-2435.2010.01802.x>, 2011.

978 Berzaghi, F., Wright, I. J., Kramer, K., Oddou-Muratorio, S., Bohn, F. J., Reyer, C. P. O., Sabate, S.,
979 Sanders, T. G. M., and Hartig, F.: Towards a new generation of trait-flexible vegetation models.
980 *Trends Ecol. Evol.*, 35, 191–205, <https://doi.org/10.1016/j.tree.2019.11.006>, 2020.

981 Blumenthal, D. M., Mueller, K. E., Kray, J. A., Ocheltree, T. W., Augustine, D. J., Wilcox, K. R.,
982 and Cornelissen, H.: Traits link drought resistance with herbivore defence and plant economics
983 in semi-arid grasslands: The central roles of phenology and leaf dry matter content. *J. Ecol.*,
984 108, 2336–2351, <https://doi.org/10.1111/1365-2745.13454>, 2020.

985 Bohner, A. Soil chemical properties as indicators of plant species richness in grassland communities.
986 Integrating efficient grassland farming and biodiversity, Proceedings of the 13th International
987 Occasional Symposium of the European Grassland Federation, Tartu, Estonia, 29–31 August,

988 48-51, 2005.

989 Boonman, C. C. F., Benitez-Lopez, A., Schipper, A. M., Thuiller, W., Anand, M., Cerabolini, B. E.
990 L., Cornelissen, J. H. C., Gonzalez-Melo, A., Hattingh, W. N., Higuchi, P., Laughlin, D. C.,
991 Onipchenko, V. G., Penuelas, J., Poorter, L., Soudzilovskaia, N. A., Huijbregts, M. A. J., and
992 Santini, L.: Assessing the reliability of predicted plant trait distributions at the global scale.
993 *Glob. Ecol. Biogeogr.*, 29, 1034–1051, <https://doi.org/10.1111/geb.13086>, 2020.

994 Breiman, L.: Random forests. *Mach. Learn.*, 45, 5–32, <https://doi.org/10.1023/a:1010933404324>,
995 2001.

996 Bruelheide, H., Dengler, J., Purschke, O., Lenoir, J., Jimenez-Alfaro, B., Hennekens, S. M., Botta-
997 Dukat, Z., Chytrý, M., Field, R., Jansen, F., Kattge, J., Pillar, V. D., Schrodte, F., Mahecha, M.
998 D., Peet, R. K., Sandel, B., van Bodegom, P., Altman, J., Alvarez-Davila, E., Arfin Khan, M.
999 A. S., et al.: Global trait-environment relationships of plant communities. *Nat. Ecol. Evol.*, 2,
1000 1906–1917, <https://doi.org/10.1038/s41559-018-0699-8>, 2018.

1001 Bruelheide, H., Dengler, J., Jiménez-Alfaro, B., Purschke, O., Hennekens, S. M., Chytrý, M., Pillar,
1002 V. D., Jansen, F., Kattge, J., Sandel, B., Aubin, I., Biurrun, I., Field, R., Haider, S., Jandt, U.,
1003 Lenoir, J., Peet, R. K., Peyre, G., Sabatini, F. M., Schmidt, M., et al.: sPlot – A new tool for
1004 global vegetation analyses. *J. Veg. Sci.*, 30, 161–186, <https://doi.org/10.1111/jvs.12710>, 2019.

1005 Buchhorn, M., Bertels, L., Smets, B., De Roo, B., Lesiv, M., Tsendbazar, N. E., Masiliunas, D., and
1006 Linlin, L.: Copernicus Global Land Service: Land Cover 100m: Version 3 Globe 2015-2019:
1007 Algorithm Theoretical Basis Document. <https://doi.org/10.5281/zenodo.3938968>, 2020.

1008 Butler, E. E., Datta, A., Flores-Moreno, H., Chen, M., Wythers, K. R., Fazayeli, F., Banerjee, A.,
1009 Atkin, O. K., Kattge, J., Amiaud, B., Blonder, B., Boenisch, G., Bond-Lamberty, B., Brown,
1010 K. A., Byun, C., Campetella, G., Cerabolini, B. E. L., Cornelissen, J. H. C., Craine, J. M.,
1011 Craven, D., de Vries, F. T., Diaz, S., Domingues, T. F., Forey, E., Gonzalez-Melo, A., Gross,
1012 N., Han, W., Hattingh, W. N., Hickler, T., Jansen, S., Kramer, K., Kraft, N. J. B., Kurokawa,
1013 H., Laughlin, D. C., Meir, P., Minden, V., Niinemets, U., Onoda, Y., Penuelas, J., Read, Q.,
1014 Sack, L., Schamp, B., Soudzilovskaia, N. A., Spasojevic, M. J., Sosinski, E., Thornton, P. E.,
1015 Valladares, F., van Bodegom, P. M., Williams, M., Wirth, C., and Reich, P. B.: Mapping local
1016 and global variability in plant trait distributions. *P. Nat. Acad. Sci. USA*, 114, 10937–10946,
1017 <https://doi.org/10.1073/pnas.1708984114>, 2017.

1018 Cavender-Bares, J., Schneider, F. D., Santos, M. J., Armstrong, A., Carnaval, A., Dahlin, K. M.,
1019 Fatoyinbo, L., Hurtt, G. C., Schimel, D., Townsend, P. A., Ustin, S. L., Wang, Z. H., and Wilson,
1020 A. M.: Integrating remote sensing with ecology and evolution to advance biodiversity
1021 conservation. *Nat. Ecol. Evol.*, 6, 506–519, <https://doi.org/10.1038/s41559-022-01702-5>, 2022.

1022 Clevers, J. G. P. W., and Gitelson, A. A.: Remote estimation of crop and grass chlorophyll and
1023 nitrogen content using red-edge bands on Sentinel-2 and -3. *Int. J. Appl. Earth Obs. Geoinf.*,
1024 23, 344–351, <https://doi.org/10.1016/j.jag.2012.10.008>, 2013.

1025 Dahlin, K. M., Asner, G. P., and Field, C. B.: Environmental and community controls on plant

1026 canopy chemistry in a Mediterranean-type ecosystem. *P. Nat. Acad. Sci. USA*, 110, 6895–6900,
1027 <https://doi.org/10.1073/pnas.1215513110>, 2013.

1028 Darvishzadeh, R., Skidmore, A., Schlerf, M., and Atzberger, C.: Inversion of a radiative transfer
1029 model for estimating vegetation LAI and chlorophyll in a heterogeneous grassland. *Remote*
1030 *Sens. Environ.*, 112, 2592–2604, <https://doi.org/10.1016/j.rse.2007.12.003>, 2008.

1031 Diaz, S., Kattge, J., Cornelissen, J. H., Wright, I. J., Lavorel, S., Dray, S., Reu, B., Kleyer, M., Wirth,
1032 C., Prentice, I. C., Garnier, E., Bonisch, G., Westoby, M., Poorter, H., Reich, P. B., Moles, A.
1033 T., Dickie, J., Gillison, A. N., Zanne, A. E., Chave, J., Wright, S. J., Sheremet'ev, S. N., Jactel,
1034 H., Baraloto, C., Cerabolini, B., Pierce, S., Shipley, B., Kirkup, D., Casanoves, F., Joswig, J.
1035 S., Gunther, A., Falczuk, V., Ruger, N., Mahecha, M. D., and Gorne, L. D.: The global spectrum
1036 of plant form and function. *Nature*, 529, 167–171, <https://doi.org/10.1038/nature16489>, 2016.

1037 Diaz, S., Hodgson, J. G., Thompson, K., Cabido, M., Cornelissen, J. H. C., Jalili, A., Montserrat-
1038 Marti, G., Grime, J. P., Zarrinkamar, F., Asri, Y., Band, S. R., Basconcelo, S., Castro-Diez, P.,
1039 Funes, G., Hamzehee, B., Khoshnevi, M., Perez-Harguindeguy, N., Perez-Rontome, M. C.,
1040 Shirvany, F. A., Vendramini, F., Yazdani, S., Abbas-Azimi, R., Bogaard, A., Boustani, S.,
1041 Charles, M., Dehghan, M., de Torres-Espuny, L., Falczuk, V., Guerrero-Campo, J., Hynd, A.,
1042 Jones, G., Kowsary, E., Kazemi-Saeed, F., Maestro-Martinez, M., Romo-Diez, A., Shaw, S.,
1043 Siavash, B., Villar-Salvador, P., and Zak, M. R.: The plant traits that drive ecosystems: evidence
1044 from three continents. *J. Veg. Sci.*, 15, 295–304, <https://doi.org/10.1111/j.1654->
1045 [1103.2004.tb02266.x](https://doi.org/10.1111/j.1654-1103.2004.tb02266.x), 2004.

1046 Dong, N., Dechant, B., Wang, H., Wright, I. J., and Prentice, IC.: Global leaf-trait mapping based
1047 on optimality theory. *Glob. Ecol. Biogeogr.*, <https://doi.org/10.1111/geb.13680>, 2023.

1048 Du, L., Liu, H., Guan, W., Li, J., and Li, J.: Drought affects the coordination of belowground and
1049 aboveground resource-related traits in *Solidago canadensis* in China. *Ecol. Evol.*, 9, 9948–
1050 9960, <https://doi.org/10.1002/ece3.5536>, 2019.

1051 Elith, J., Leathwick, J. R., and Hastie, T.: A working guide to boosted regression trees. *J. Anim.*
1052 *Ecol.*, 77, 802–813, <https://doi.org/10.1111/j.1365-2656.2008.01390.x>, 2008.

1053 Elith, J., Kearney, M., and Phillips, S.: The art of modelling range-shifting species. *Methods Ecol.*
1054 *Evol.*, 1, 330–342, <https://doi.org/10.1111/j.2041-210X.2010.00036.x>, 2010.

1055 Elith, J., Graham, C. H., Anderson, R. P., Dudik, M., Ferrier, S., Guisan, A., Hijmans, R. J.,
1056 Huettmann, F., Leathwick, J. R., Lehmann, A., Li, J., Lohmann, L. G., Loiselle, B. A., Manion,
1057 G., Moritz, C., Nakamura, M., Nakazawa, Y., Overton, J. M., Peterson, A. T., Phillips, S. J.,
1058 Richardson, K., Scachetti-Pereira, R., Schapire, R. E., Soberon, J., Williams, S., Wisz, M. S.,
1059 and Zimmermann, N. E.: Novel methods improve prediction of species' distributions from
1060 occurrence data. *Ecography*, 29, 129–151, <https://doi.org/10.1111/j.2006.0906-7590.04596.x>,
1061 2006.

1062 Finzi, A. C., Austin, A. T., Cleland, E. E., Frey, S. D., Houlton, B. Z., and Wallenstein, M. D.:
1063 Responses and feedbacks of coupled biogeochemical cycles to climate change: examples from

1064 terrestrial ecosystems. *Front. Ecol. Environ.*, 9, 61–67, <https://doi.org/10.1890/100001>, 2011.

1065 Foley, J. A., Prentice, I. C., Ramankutty, N., Levis, S., Pollard, D., Sitch, S., and Haxeltine, A.: An
1066 integrated biosphere model of land surface processes, terrestrial carbon balance, and vegetation
1067 dynamics. *Global Biogeochem. Cy.*, 10, 603–628, <https://doi.org/10.1029/96gb02692>, 1996.

1068 Freschet, G. T., Cornelissen, J. H. C., van Logtestijn, R. S. P., and Aerts, R.: Evidence of the ‘plant
1069 economics spectrum’ in a subarctic flora. *J. Ecol.*, 98, 362–373, <https://doi.org/10.1111/j.1365-2745.2009.01615.x>, 2010.

1071 Grime, J. P.: Benefits of plant diversity to ecosystems: immediate, filter and founder effects. *J. Ecol.*,
1072 86, 902–910, <https://doi.org/10.1046/j.1365-2745.1998.00306.x>, 1998.

1073 He, N., Yan, P., Liu, C., Xu, L., Li, M., Van Meerbeek, K., Zhou, G., Zhou, G., Liu, S., Zhou, X.,
1074 Li, S., Niu, S., Han, X., Buckley, T. N., Sack, L., and Yu, G.: Predicting ecosystem productivity
1075 based on plant community traits. *Trends Plant Sci.*, 28, 43–53,
1076 <https://doi.org/10.1016/j.tplants.2022.08.015>, 2023.

1077 Hodgson, J. G., Montserrat-Marti, G., Charles, M., Jones, G., Wilson, P., Shipley, B., Sharafi, M.,
1078 Cerabolini, B. E. L., Cornelissen, J. H. C., Band, S. R., Bogard, A., Castro-Diez, P., Guerrero-
1079 Campo, J., Palmer, C., Perez-Rontome, M. C., Carter, G., Hynd, A., Romo-Diez, A., Espuny,
1080 L. D., and Pla, F. R.: Is leaf dry matter content a better predictor of soil fertility than specific
1081 leaf area? *Ann. Bot.*, 108, 1337–1345, <https://doi.org/10.1093/aob/mcr225>, 2011.

1082 Hoeber, S., Leuschner, C., Köhler, L., Arias-Aguilar, D., and Schuldt, B.: The importance of
1083 hydraulic conductivity and wood density to growth performance in eight tree species from a
1084 tropical semi-dry climate. *Forest Ecol. Manag.*, 330, 126–136,
1085 <https://doi.org/10.1016/j.foreco.2014.06.039>, 2014.

1086 Jónsdóttir, I. S., Halbritter, A. H., Christiansen, C. T., Althuisen, I. H. J., Haugum, S. V., Henn, J. J.,
1087 Björnsdóttir, K., Maitner, B. S., Malhi, Y., Michaletz, S. T., Roos, R. E., Klanderud, K., Lee,
1088 H., Enquist, B. J., and Vandvik, V.: Intraspecific trait variability is a key feature underlying
1089 high Arctic plant community resistance to climate warming. *Ecol. Monogr.*, 93,
1090 <https://doi.org/10.1002/ecm.1555>, 2022.

1091 Jung, V., Violle, C., Mondy, C., Hoffmann, L., and Muller, S.: Intraspecific variability and trait-
1092 based community assembly. *J. Ecol.*, 98, 1134–1140, <https://doi.org/10.1111/j.1365-2745.2010.01687.x>, 2010.

1094 Kattge, J., Diaz, S., Lavorel, S., Prentice, C., Leadley, P., Bonisch, G., Garnier, E., Westoby, M.,
1095 Reich, P. B., Wright, I. J., Cornelissen, J. H. C., Violle, C., Harrison, S. P., van Bodegom, P. M.,
1096 Reichstein, M., Enquist, B. J., Soudzilovskaia, N. A., Ackerly, D. D., Anand, M., Atkin, O., et
1097 al.: TRY - a global database of plant traits. *Glob. Change Biol.*, 17, 2905–2935,
1098 <https://doi.org/10.1111/j.1365-2486.2011.02451.x>, 2011.

1099 Kattge, J., Bonisch, G., Diaz, S., Lavorel, S., Prentice, I. C., Leadley, P., Tautenhahn, S., Werner, G.
1100 D. A., Aakala, T., Abedi, M., Acosta, A. T. R., Adamidis, G. C., Adamson, K., Aiba, M., Albert,
1101 C. H., Alcantara, J. M., Alcazar, C. C., Aleixo, I., Ali, H., Amiaud, B., et al.: TRY plant trait

1102 database - enhanced coverage and open access. *Global Change Biol.*, 26, 119–188,
1103 <https://doi.org/10.1111/gcb.14904>, 2020.

1104 King, D. A., Davies, S. J., Tan, S., and Noor, N. S. M.: The role of wood density and stem support
1105 costs in the growth and mortality of tropical trees. *J. Ecol.*, 94, 670–680,
1106 <https://doi.org/10.1111/j.1365-2745.2006.01112.x>, 2006.

1107 Kirilenko, A. P., Belotelov, N. V., and Bogatyrev, B. G.: Global model of vegetation migration:
1108 incorporation of climatic variability. *Ecol. Model.*, 132, 125–133,
1109 [https://doi.org/10.1016/S0304-3800\(00\)00310-0](https://doi.org/10.1016/S0304-3800(00)00310-0), 2000.

1110 LeBauer, D. S., and Treseder, K. K.: Nitrogen limitation of net primary productivity in terrestrial
1111 ecosystems is globally distributed. *Ecology*, 89, 371–379, <https://doi.org/10.1890/06-2057.1>,
1112 2008.

1113 Li, C. X., Wulf, H., Schmid, B., He, J. S., and Schaepman, M. E.: Estimating plant traits of alpine
1114 grasslands on the Qinghai-Tibetan Plateau using remote sensing. *IEEE J. Sel. Top. Appl. Earth
1115 Obs. Remote Sens.*, 11, 2263–2275, <https://doi.org/10.1109/jstars.2018.2824901>, 2018.

1116 Li, D. J., Ives, A. R., and Waller, D. M.: Can functional traits account for phylogenetic signal in
1117 community composition? *New Phytol.*, 214, 607–618, <https://doi.org/10.1111/nph.14397>,
1118 2017.

1119 Li, Y. Q., Reich, P. B., Schmid, B., Shrestha, N., Feng, X., Lyu, T., Maitner, B. S., Xu, X., Li, Y. C.,
1120 Zou, D. T., Tan, Z. H., Su, X. Y., Tang, Z. Y., Guo, Q. H., Feng, X. J., Enquist, B. J., and Wang,
1121 Z. H.: Leaf size of woody dicots predicts ecosystem primary productivity. *Ecol. Lett.*, 23, 1003–
1122 1013, <https://doi.org/10.1111/ele.13503>, 2020.

1123 Liang, X. Y., Ye, Q., Liu, H., and Brodribb, T. J.: Wood density predicts mortality threshold for
1124 diverse trees. *New Phytol.*, 229, <https://doi.org/10.1111/nph.17117>, 2021.

1125 Liaw, A., and Wiener, M.: Classification and Regression by randomForest. *R News*, 2, 18–22, 2002.

1126 Liu, H. Y., and Yin, Y.: Response of forest distribution to past climate change: an insight into future
1127 predictions. *Chinese Science Bulletin*, 58, 4426–4436, <https://doi.org/10.1007/s11434-013-6032-7>,
1128 2013.

1129 Loozen, Y., Rebel, K. T., Karssenber, D., Wassen, M. J., Sardans, J., Peñuelas, J., and De Jong, S.
1130 M.: Remote sensing of canopy nitrogen at regional scale in Mediterranean forests using the
1131 spaceborne MERIS Terrestrial Chlorophyll Index. *Biogeosciences*, 15, 2723–2742,
1132 <https://doi.org/10.5194/bg-15-2723-2018>, 2018.

1133 Loozen, Y., Rebel, K. T., de Jong, S. M., Lu, M., Ollinger, S. V., Wassen, M. J., and Karssenber,
1134 D.: Mapping canopy nitrogen in European forests using remote sensing and environmental
1135 variables with the random forests method. *Remote Sens. Environ.*, 247, 111933,
1136 <https://doi.org/10.1016/j.rse.2020.111933>, 2020.

1137 Madani, N., Kimball, J. S., Ballantyne, A. P., Affleck, D. L. R., van Bodegom, P. M., Reich, P. B.,
1138 Kattge, J., Sala, A., Nazeri, M., Jones, M. O., Zhao, M., and Running, S. W.: Future global
1139 productivity will be affected by plant trait response to climate. *Sci. Rep.*, 8, 1–10,

1140 <https://doi.org/10.1038/s41598-018-21172-9>, 2018.

1141 Martínez-Vilalta, J., Mencuccini, M., Vayreda, J., and Retana, J.: Interspecific variation in functional
1142 traits, not climatic differences among species ranges, determines demographic rates across 44
1143 temperate and Mediterranean tree species. *J. Ecol.*, 98, 1462–1475,
1144 <https://doi.org/10.1111/j.1365-2745.2010.01718.x>, 2010.

1145 Matheny, A. M., Mirfenderesgi, G., and Bohrer, G.: Trait-based representation of hydrological
1146 functional properties of plants in weather and ecosystem models. *Plant Divers*, 39, 1–12,
1147 <https://doi.org/10.1016/j.pld.2016.10.001>, 2017.

1148 Moles, A. T., Warton, D. I., Warman, L., Swenson, N. G., Laffan, S. W., Zanne, A. E., Pitman, A.,
1149 Hemmings, F. A., and Leishman, M. R.: Global patterns in plant height. *J. Ecol.*, 97, 923–932,
1150 <https://doi.org/10.1111/j.1365-2745.2009.01526.x>, 2009.

1151 Moreno-Martínez, Á., Camps-Valls, G., Kattge, J., Robinson, N., Reichstein, M., van Bodegom, P.,
1152 Kramer, K., Cornelissen, J. H. C., Reich, P., Bahn, M., Niinemets, Ü., Peñuelas, J., Craine, J.
1153 M., Cerabolini, B. E. L., Minden, V., Laughlin, D. C., Sack, L., Allred, B., Baraloto, C., Byun,
1154 C., Soudzilovskaia, N. A., and Running, S. W.: A methodology to derive global maps of leaf
1155 traits using remote sensing and climate data. *Remote Sens. Environ.*, 218, 69–88,
1156 <https://doi.org/10.1016/j.rse.2018.09.006>, 2018.

1157 Myers-Smith, I. H., Thomas, H. J. D., and Bjorkman, A. D.: Plant traits inform predictions of tundra
1158 responses to global change. *New Phytol.*, 221, 1742–1748, <https://doi.org/10.1111/nph.15592>,
1159 2019.

1160 NEODC, 2015. NEODC - NERC Earth Observation Data Centre. Natural Environment Research
1161 Council. <http://neodc.nerc.ac.uk/>.

1162 Peng, C. H.: From static biogeographical model to dynamic global vegetation model: a global
1163 perspective on modelling vegetation dynamics. *Ecol. Model.*, 135, 33–54,
1164 [https://doi.org/10.1016/S0304-3800\(00\)00348-3](https://doi.org/10.1016/S0304-3800(00)00348-3), 2000.

1165 Perez-Harguindeguy, N., Diaz, S., Garnier, E., Lavorel, S., Poorter, H., Jaureguiberry, P., Bret-Harte,
1166 M. S., Cornwell, W. K., Craine, J. M., Gurvich, D. E., Urcelay, C., Veneklaas, E. J., Reich, P.
1167 B., Poorter, L., Wright, I. J., Ray, P., Enrico, L., Pausas, J. G., de Vos, A. C., Buchmann, N.,
1168 Funes, G., Quetier, F., Hodgson, J. G., Thompson, K., Morgan, H. D., ter Steege, H., van der
1169 Heijden, M. G. A., Sack, L., Blonder, B., Poschlod, P., Vaieretti, M. V., Conti, G., Staver, A. C.,
1170 Aquino, S., and Cornelissen, J. H. C.: New handbook for standardised measurement of plant
1171 functional traits worldwide. *Aust. Bot.*, 61, 167–234, <https://doi.org/10.1071/bt12225>, 2013.

1172 Piao, S. L., He, Y., Wang, X. H., and Chen, F. H.: Estimation of China’s terrestrial ecosystem carbon
1173 sink: Methods, progress and prospects. *Science China Earth Sciences*, 65, 641–651,
1174 <https://doi.org/10.1007/s11430-021-9892-6>, 2022.

1175 Potapov, P., Li, X. Y., Hernandez-Serna, A., Tyukavina, A., Hansen, M. C., Kommareddy, A.,
1176 Pickens, A., Turubanova, S., Tang, H., Silva, C. E., Armston, J., Dubayah, R., Blair, J. B.,
1177 Hofton, M.: Mapping global forest canopy height through integration of GEDI and Landsat

1178 data, *Remote Sens. Environ.*, 253, 112165, <https://doi.org/10.1016/j.rse.2020.112165>, 2021.

1179 Qiao, J. J., Zuo, X. A., Yue, P., Wang, S. K., Hu, Y., Guo, X. X., Li, X. Y., Lv, P., Guo, A. X., and
1180 Sun, S. S.: High nitrogen addition induces functional trait divergence of plant community in a
1181 temperate desert steppe. *Plant and Soil*, <https://doi.org/10.1007/s11104-023-05910-1>, 2023.

1182 Reich, P. B., and Oleksyn, J.: Global patterns of plant leaf N and P in relation to temperature and
1183 latitude. *Proc. Natl. Acad. Sci. U. S. A.*, 101, 11001–11006,
1184 https://doi.org/10.1073/pnas.0403588101_2004.

1185 Reich, P. B., and Cornelissen, H.: The world-wide ‘fast-slow’ plant economics spectrum: a traits
1186 manifesto. *Journal of Ecology*, 102, 275–301, <https://doi.org/10.1111/1365-2745.12211>, 2014.

1187 Reich, P. B., Uhl, C., Walters, M. B., and Ellsworth, D. S.: Leaf lifespan as a determinant of leaf
1188 structure and function among 23 Amazonian tree species. *Oecologia*, 86, 16–24,
1189 <https://doi.org/10.1007/BF00317383>, 1991.

1190 Ridgeway, G.: Gbm: generalized boosted regression models. R package version 1.5-6, Available at:
1191 <http://cran.r-project.org/web/packages/gbm/index.html>, accessed 11/02/20092006.

1192 Roderick, M. L., and Berry, S. L.: Linking wood density with tree growth and environment: a
1193 theoretical analysis based on the motion of water. *New Phytol.*, 149, 473–485,
1194 <https://doi.org/10.1046/j.1469-8137.2001.00054.x>, 2002.

1195 Romero, A., Aguado, I., and Yebra, M.: Estimation of dry matter content in leaves using normalized
1196 indexes and PROSPECT model inversion. *Int. J. Remote Sens.*, 33, 396–414,
1197 <https://doi.org/10.1080/01431161.2010.532819>, 2012.

1198 Sakschewski, B., von Bloh, W., Boit, A., Rammig, A., Kattge, J., Poorter, L., Penuelas, J., and
1199 Thonicke, K.: Leaf and stem economics spectra drive diversity of functional plant traits in a
1200 dynamic global vegetation model. *Global Change Biol.*, 21, 2711–2725,
1201 https://doi.org/10.1111/gcb.12870_2015.

1202 Scheiter, S., Langan, L., and Higgins, S. I.: Next-generation dynamic global vegetation models:
1203 learning from community ecology. *New Phytol.*, 198, 957–969,
1204 <https://doi.org/10.1111/nph.12210>, 2013.

1205 Schiller, C., Schmidtlein, S., Boonman, C., Moreno-Martinez, A., and Kattenborn, T.: Deep learning
1206 and citizen science enable automated plant trait predictions from photographs. *Sci. Rep.*, 11,
1207 <https://doi.org/10.1038/s41598-021-95616-0>, 2022.

1208 Shangguan, W., Dai, Y. J., Liu, B. Y., Zhu, A. X., Duan, Q. Y., Wu, L. Z., Ji, D. Y., Ye, A. Z., Yuan,
1209 H., Zhang, Q., Chen, D. D., Chen, M., Chu, J. T., Dou, Y. J., Guo, J. X., Li, H. Q., Li, J. J.,
1210 Liang, L., Liang, X., Liu, H. P., Liu, S. Y., Miao, C. Y., and Zhang, Y. Z.: A China data set of
1211 soil properties for land surface modeling. *J. Adv. Model. Earth Syst.*, 5, 212–224,
1212 <https://doi.org/10.1002/jame.20026>, 2013.

1213 Siefert, A., Violle, C., Chalmandrier, L., Albert, C. H., Taudiere, A., Fajardo, A., Aarssen, L. W.,
1214 Baraloto, C., Carlucci, M. B., Cianciaruso, M. V., de, L. D. V., de Bello, F., Duarte, L. D.,
1215 Fonseca, C. R., Freschet, G. T., Gaucherand, S., Gross, N., Hikosaka, K., Jackson, B., Jung, V.,

1216 Kamiyama, C., Katabuchi, M., Kembel, S. W., Kichenin, E., Kraft, N. J., Lagerstrom, A.,
1217 Bagousse-Pinguet, Y. L., Li, Y., Mason, N., Messier, J., Nakashizuka, T., Overton, J. M., Peltzer,
1218 D. A., Perez-Ramos, I. M., Pillar, V. D., Prentice, H. C., Richardson, S., Sasaki, T., Schamp, B.
1219 S., Schob, C., Shipley, B., Sundqvist, M., Sykes, M. T., Vandewalle, M., and Wardle, D. A.: A
1220 global meta-analysis of the relative extent of intraspecific trait variation in plant communities.
1221 *Ecol. Lett.*, 18, 1406–1419, <https://doi.org/10.1111/ele.12508>, 2015.

1222 Šímová, I., Sandel, B., Enquist, B. J., Michaletz, S. T., Kattge, J., Violle, C., McGill, B. J., Blonder,
1223 B., Engemann, K., Peet, R. K., Wiser, S. K., Morueta-Holme, N., Boyle, B., Kraft, N. J. B.,
1224 Svenning, J. C., and Hector, A.: The relationship of woody plant size and leaf nutrient content
1225 to large-scale productivity for forests across the Americas. *J. Ecol.*, 107, 2278–2290,
1226 <https://doi.org/10.1111/1365-2745.13163>, 2019.

1227 Sitch, S., Huntingford, C., Gedney, N., Levy, P. E., Lomas, M., Piao, S. L., Betts, R., Ciais, P., Cox,
1228 P., Friedlingstein, P., Jones, C. D., Prentice, I. C., and Woodward, F. I.: Evaluation of the
1229 terrestrial carbon cycle, future plant geography and climate-carbon cycle feedbacks using five
1230 Dynamic Global Vegetation Models (DGVMs). *Global Change Biol.*, 14, 2015–2039,
1231 <https://doi.org/10.1111/j.1365-2486.2008.01626.x>, 2008.

1232 Smart, S. M., Glanville, H. C., Blanes, M. d. C., Mercado, L. M., Emmett, B. A., Jones, D. L., Cosby,
1233 B. J., Marrs, R. H., Butler, A., Marshall, M. R., Reinsch, S., Herrero-Jáuregui, C., Hodgson, J.
1234 G., and Field, K.: Leaf dry matter content is better at predicting above-ground net primary
1235 production than specific leaf area. *Funct. Ecol.*, 31, 1336–1344, <https://doi.org/10.1111/1365-2435.12832>, 2017.

1237 Telenius, A.: Biodiversity information goes public: GBIF at your service. *Nord. J. Bot.*, 29, 378–
1238 381, <https://doi.org/10.1111/j.1756-1051.2011.01167.x>, 2011.

1239 Thomas, D. S., Montagu, K. D., and Conroy, J. P.: Changes in wood density of *Eucalyptus*
1240 *camaldulensis* due to temperature—the physiological link between water viscosity and wood
1241 anatomy. *Forest Ecol. Manag.*, 193, 157–165, <https://doi.org/10.1016/j.foreco.2004.01.028>,
1242 2004.

1243 Thomas, S. C.: Photosynthetic capacity peaks at intermediate size in temperate deciduous trees. *Tree*
1244 *Physiol.*, 30, 555–573, <https://doi.org/10.1093/treephys/tpq005>, 2010.

1245 Thuiller, W., Lafourcade, B., Engler, R., and Araújo, M. B.: BIOMOD – A platform for ensemble
1246 forecasting of species distributions. *Ecography*, 32, 369–373, <https://doi.org/10.1111/j.1600-0587.2008.05742.x>, 2009.

1248 Trabucco, A., and Zomer, R. J.: Global Aridity Index and Potential Evapo-Transpiration (ET0)
1249 Climate Database v2. CGIAR Consortium for Spatial Information (CGIAR-CSI),
1250 <https://cgiarcsi.community>, 2018.

1251 Vallicrosa, H., Sardans, J., Maspons, J., Zuccarini, P., Fernández-Martínez, M., Bauters, M., Goll,
1252 D. S., Ciais, P., Obersteiner, M., Janssens, I. A., and Peñuelas, J.: Global maps and factors
1253 driving forest foliar elemental composition: the importance of evolutionary history. *New*

1254 Phytol., 233, 169–181, <https://doi.org/10.1111/nph.17771>, 2022.

1255 Van Bodegom, P. M., Douma, J. C., Witte, J. P. M., Ordoñez, J. C., Bartholomeus, R. P., and Aerts,
1256 R.: Going beyond limitations of plant functional types when predicting global ecosystem-
1257 atmosphere fluxes: exploring the merits of traits-based approaches. *Glob. Ecol. Biogeogr.*, 21,
1258 625–636, <https://doi.org/10.1111/j.1466-8238.2011.00717.x>, 2012.

1259 van Bodegom, P. M., Douma, J. C., and Verheijen, L. M. A fully traits-based approach to modeling
1260 global vegetation distribution. *P. Nat. Acad. Sci. USA*, 111, 13733–13738,
1261 <https://doi.org/10.1073/pnas.1304551110>, 2014.

1262 Verheijen, L. M., Aerts, R., Bonisch, G., Kattge, J., and Van Bodegom, P. M.: Variation in trait trade-
1263 offs allows differentiation among predefined plant functional types: implications for predictive
1264 ecology. *New Phytol.*, 209, 563–575, <https://doi.org/10.1111/nph.13623>, 2016.

1265 Wang, H., Harrison, S. P., Prentice, I. C., Yang, Y. Z., Bai, F., Togashi, H. F., Wang, M., Zhou, S. X.,
1266 and Ni, J.: The China Plant Trait Database: toward a comprehensive regional compilation of
1267 functional traits for land plants. *Ecology*, 99, 500, <https://doi.org/10.1002/ecy.2091>, 2018.

1268 Webb, C. T., Hoeting, J. A., Ames, G. M., Pyne, M. I., and LeRoy Poff, N.: A structured and dynamic
1269 framework to advance traits-based theory and prediction in ecology. *Ecol. Lett.*, 13, 267–283,
1270 <https://doi.org/10.1111/j.1461-0248.2010.01444.x>, 2010.

1271 Wright, I. J., Dong, N., Maire, V., Prentice, I. C., Westoby, M., Diaz, S., Gallagher, R. V., Jacobs, B.
1272 F., Kooyman, R., Law, E. A., Leishman, M. R., Niinemets, U., Reich, P. B., Sack, L., Villar, R.,
1273 Wang, H., and Wilf, P.: Global climatic drivers of leaf size. *Science*, 357, 917–921,
1274 <https://doi.org/10.1126/science.aal4760>, 2017.

1275 Wright, I. J., Reich, P. B., Westoby, M., Ackerly, D. D., Baruch, Z., Bongers, F., Cavender-Bares, J.,
1276 Chapin, T., Cornelissen, J. H. C., Diemer, M., Flexas, J., Garnier, E., Groom, P. K., Gulias, J.,
1277 Hikosaka, K., Lamont, B. B., Lee, T., Lee, W., Lusk, C., Midgley, J. J., Navas, M. L., Niinemets,
1278 U., Oleksyn, J., Osada, N., Poorter, H., Poot, P., Prior, L., Pyankov, V. I., Roumet, C., Thomas,
1279 S. C., Tjoelker, M. G., Veneklaas, E. J., and Villar, R.: The worldwide leaf economics spectrum.
1280 *Nature*, 428, 821–827, <https://doi.org/10.1038/nature02403>, 2004.

1281 Wullschleger, S. D., Epstein, H. E., Box, E. O., Euskirchen, E. S., Goswami, S., Iversen, C. M.,
1282 Kattge, J., Norby, R. J., van Bodegom, P. M., and Xu, X.: Plant functional types in earth system
1283 models: past experiences and future directions for application of dynamic vegetation models
1284 in high-latitude ecosystems. *Ann. Bot.*, 114, 1–16, <https://doi.org/10.1093/aob/mcu077>, 2014.

1285 Yan, P., He, N. P., Yu, K. L., Xu, L., and Van Meerbeek, K.: Integrating multiple plant functional
1286 traits to predict ecosystem productivity. *Commun Biol*, 6, 239, <https://doi.org/10.1038/s42003-023-04626-3>, 2023.

1288 Yang, Y. Z., Zhu, Q. A., Peng, C. H., Wang, H., Xue, W., Lin, G. H., Wen, Z. M., Chang, J., Wang,
1289 M., Liu, G. B., and Li, S. Q.: A novel approach for modelling vegetation distributions and
1290 analysing vegetation sensitivity through trait-climate relationships in China. *Sci. Rep.*, 6, 24110,
1291 <https://doi.org/10.1038/srep24110>, 2016.

1292 Yang, Y. Z., Wang, H., Harrison, S. P., Prentice, I. C., Wright, I. J., Peng, C. H., and Lin, G. H.:
1293 Quantifying leaf-trait covariation and its controls across climates and biomes. *New Phytol.*,
1294 221, 155-168, <https://doi.org/10.1111/nph.15422>, 2018.

1295 Yang, Y. Z., Zhao, J., Zhao, P. X., Wang, H., Wang, B. H., Su, S. F., Li, M. X., Wang, L. M., Zhu,
1296 Q. A., Pang, Z. Y., and Peng, C. H.: Trait-Based Climate Change Predictions of Vegetation
1297 Sensitivity and Distribution in China. *Front. Plant Sci.*, 10, 908,
1298 <https://doi.org/10.3389/fpls.2019.00908>, 2019.

1299 Yurova, A. Y., and Volodin, E. M.: Coupled simulation of climate and vegetation dynamics. *Izv.,*
1300 *Atmos. . Ocean. Phy.*, 47, 531-539, <https://doi.org/10.1134/s0001433811050124>, 2011.

1301 Zaehle, S., and Friend, A. D.: Carbon and nitrogen cycle dynamics in the O-CN land surface model:
1302 1. Model description, site-scale evaluation, and sensitivity to parameter estimates. *Global*
1303 *Biogeochem. Cy.*, 24, n/a-n/a, <https://doi.org/10.1029/2009gb003521>, 2010.